

third lecture

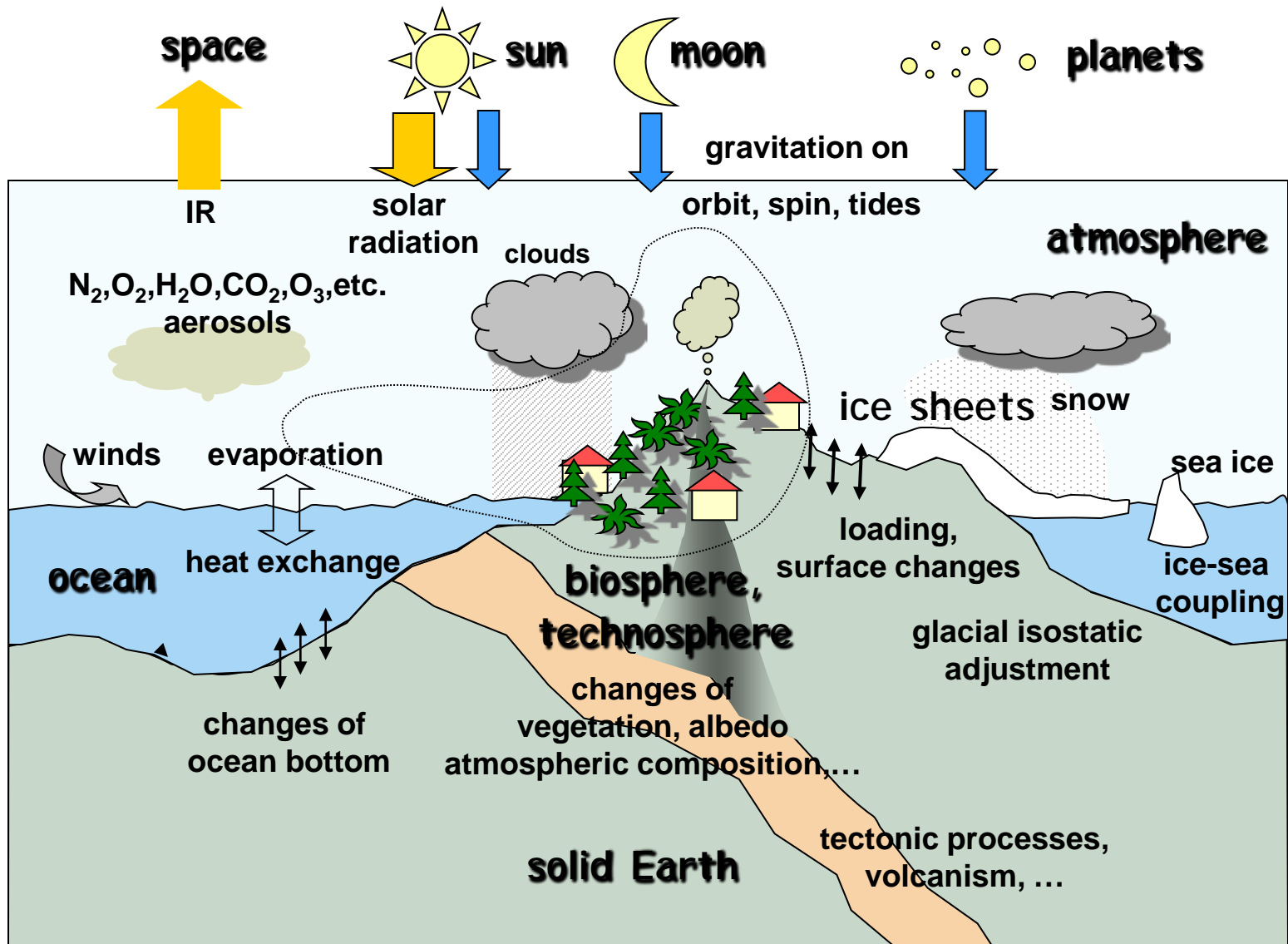
Three Lectures:

One ESA explorer mission GOCE: earth gravity from space

Two Signal Processing on a sphere

Three Gravity and earth sciences

Earth system



after Kandel, 1980

gravity and earth system science

There are three ways to use gravity in earth system sciences

1. Temporal variations of geoid/gravity
2. Geoid/gravity as a measure of mass imbalance
3. Geoid as a physically relevant reference surface

gravity and earth system science

Usage One:

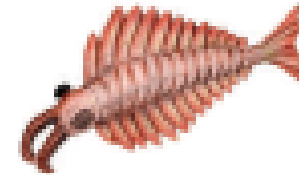
Temporal variations caused by re-distribution of masses in earth system:

- atmospheric masses
- continental water cycle
- sea level rise: steric effect vs. mass effect
- ice melting: Greenland, Antarctica, glaciers
- post-glacial adjustment
- earthquakes

Challenges:

- separation of effects (use: background models)
- aliasing (use: background models)
- spatial resolution

Satellite mission GRACE (2002 – present)



CAMBRIAN HUNTER DEFANGED

Animals can't hunt if they don't have the chops to chew up trilobites.
www.nature.com/news

PHOTO: MICHAEL GOODMAN

Satellite data show Indian water stocks shrinking

Unsustainable water use in India is threatening agricultural production and raising the spectre of a major water crisis.

Matthew Rodell of NASA's Goddard Space Flight Center in Greenbelt, Maryland, and colleagues used data from the Gravity Recovery and Climate Experiment (GRACE) satellite — operated by NASA and the German Aerospace Center (DLR) — to determine

how ground-water levels are changing in the Indian states of Rajasthan, Punjab and Haryana, which includes the national capital of New Delhi.

Their research, published online in *Nature* this week (M. Rodell et al. *Nature* doi:10.1038/nature08238, 2009), found gravity anomalies suggesting a net loss of 109 cubic kilometres of water — equivalent to a mass of 109 billion tonnes — from August 2002 to October 2008.

"If farmers could shift away from water-intensive crops and implement more efficient irrigation methods, that would help."

The amount lost is double the capacity of India's largest surface-water reservoir, the Upper Wainganga, and almost three times the capacity of Lake Mead in Nevada, the largest reservoir in the United States.

A second study using GRACE data, by scientists at the University of Colorado and the National Center for Atmospheric Research in Boulder, has found that the most intensively irrigated areas in northern India,

eastern Pakistan and parts of Bangladesh are losing groundwater at an overall rate of 54 cubic kilometres per year, consistent with Rodell's results (V.M. Tevari et al. *Geophys. Res. Lett.* doi:10.1029/2009GL039401; in the press).

Groundwater depletion in north-west India is a known problem, but Rodell's data suggest that the loss rate is around 30% higher than the Indian authorities have previously estimated.

Rodell notes that rainfall during the

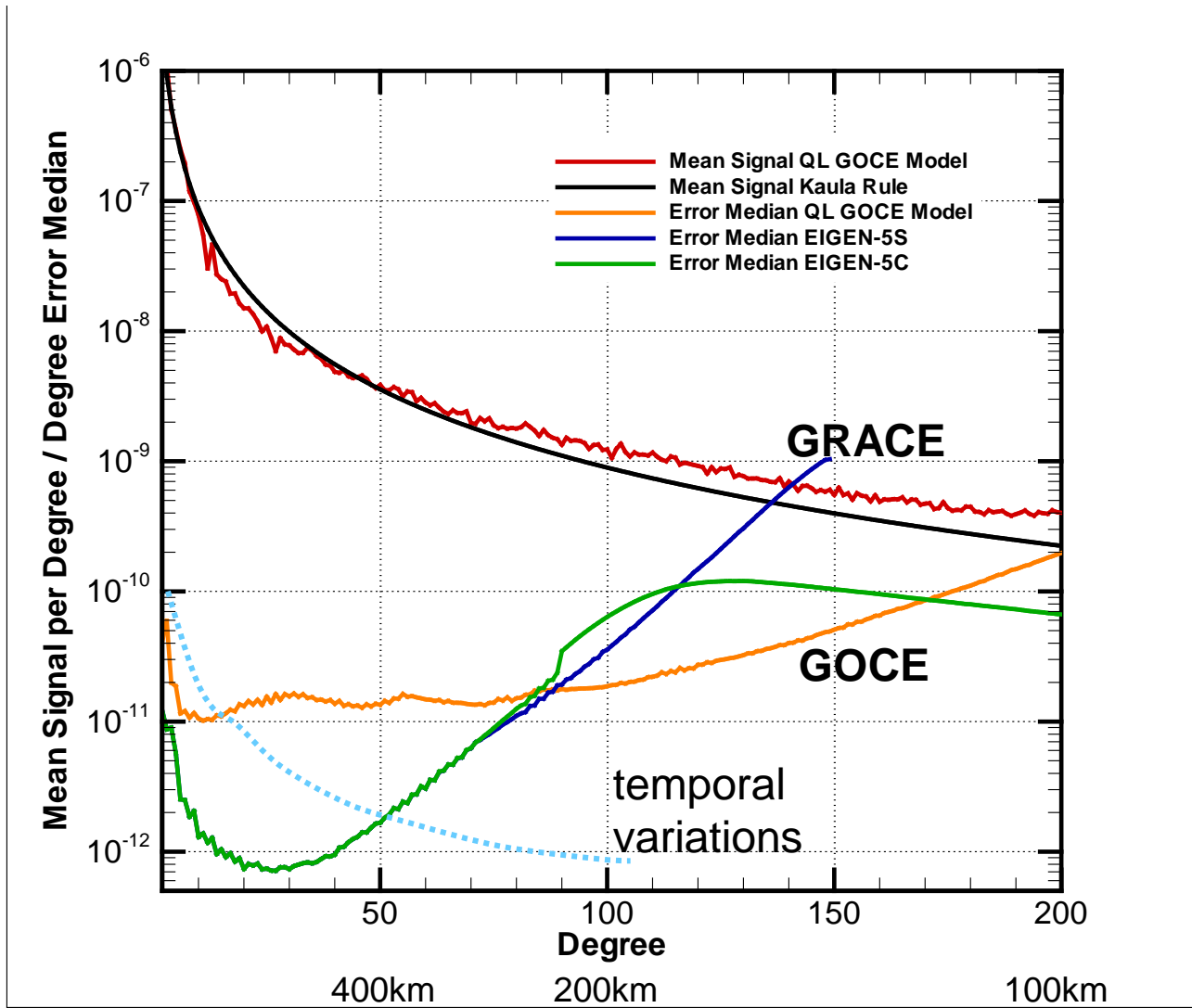
study period was close to the long-term climatic mean, and says that the observed ground-water depletion is unlikely to be the result of unusual dryness or variability.

The regions of Rajasthan, Punjab and Haryana have a combined population of 114 million people, and receive an average of 500 millimetres of rainfall per year — just slightly less than that of London — but with pronounced seasonal and regional differences. Although less than a third of agricultural land there is irrigated, crop irrigation accounts for up to 95% of ground-water consumption. "If farmers could shift away from water-intensive crops, such as rice, and implement more efficient irrigation methods, that would help," says Rodell.

Meanwhile, the Indian government is looking into framing regulations to reduce ground-water consumption. "Hop to it," says Rodell, "our research will give them the evidence they need to carry through."

Quirin Schiermeier

GOCE versus GRACE



degree variances (median) of signal and noise

gravity and earth system science

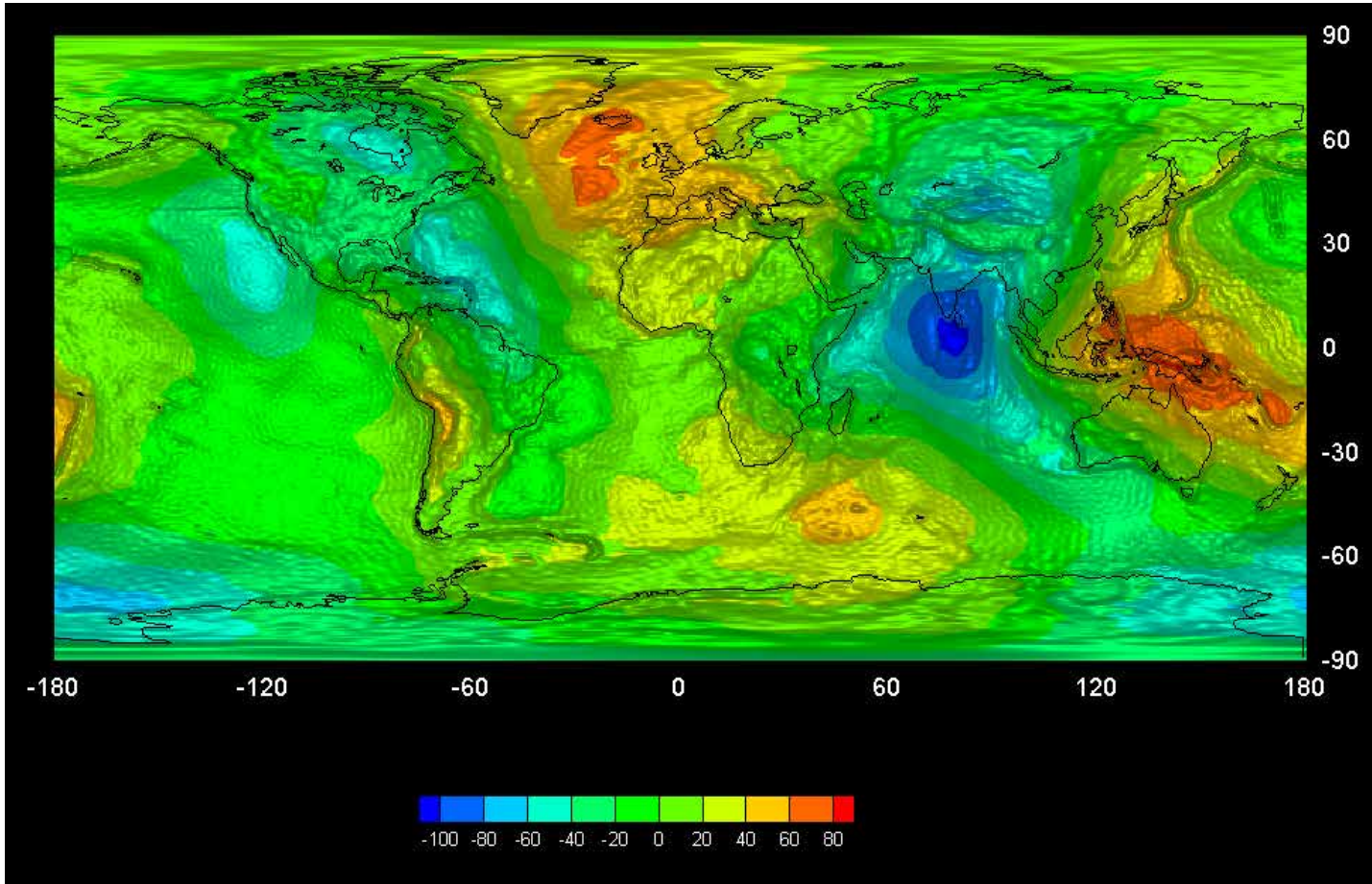
Usage Two

geoid and/or gravity as a measure of mass imbalance

- deviation of the geoid from a hydrostatic equilibrium figure
- geoid and/or gravity anomalies compared to various models of isostasy (mass balance)
- gravity inversion jointly with seismic tomography

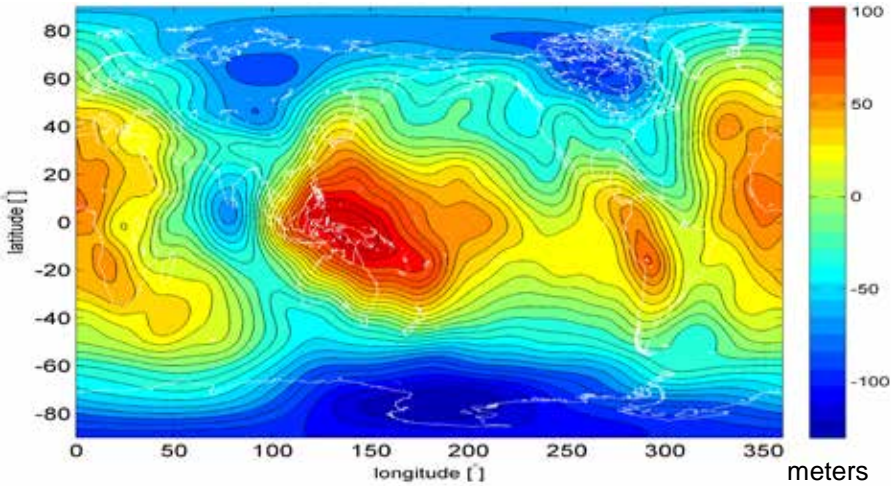
from gravity to geodynamics

a global geoid map based on two months of GOCE data



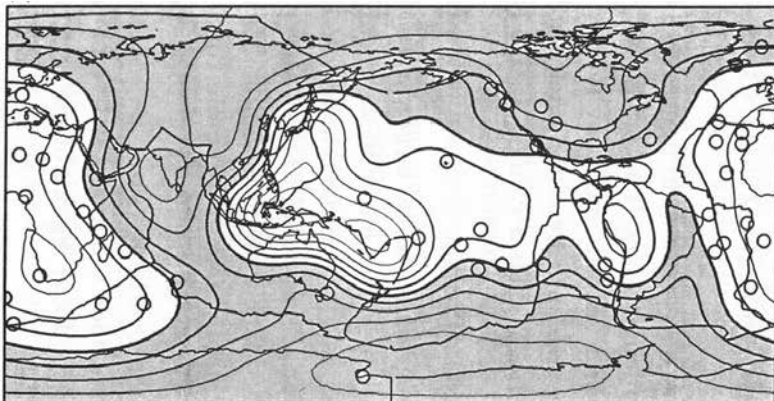
what do we see at large scales and at short scales?

from gravity to geodynamics



What do we see at large scales ?

- little resemblance to topography and tectonic plates
- geoid highs at convergence zones and concentrations of hot spots
- only at convergence zones association with topography/ plates
- primary source of large scales: deep mantle convection



Richards & Hager, 1988

Hager and Richards, 1989

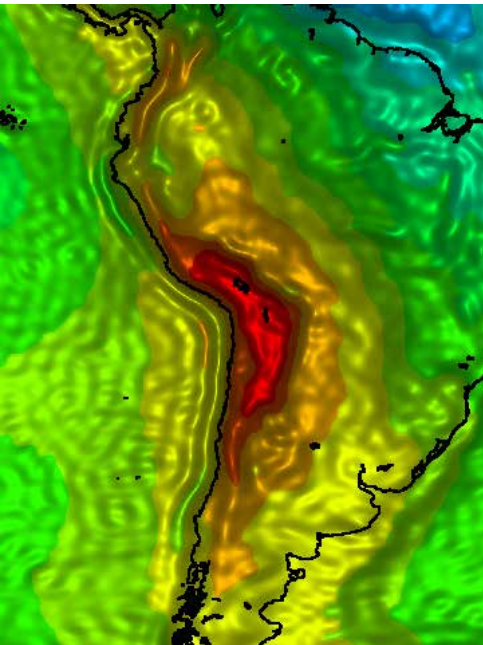
from gravity to geodynamics



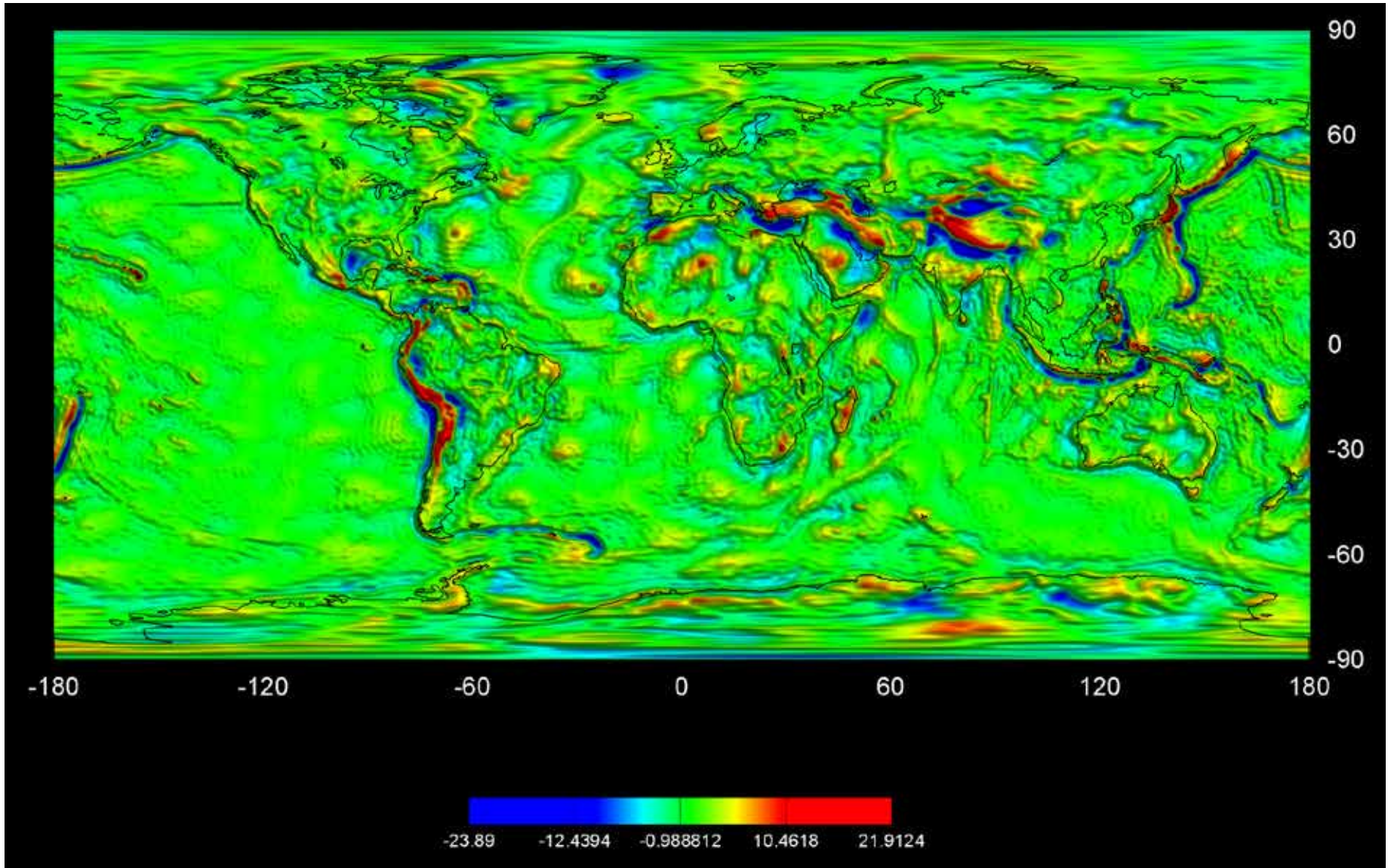
USGS: Seismicity
of the Earth 1900-2007
Nazca Plate and South America

What do we see at short scales ?

- at first sight gravity anomalies resemble topographic heights
- a closer look reveals: gravity anomalies as derived from topography show marked differences to the observed ones
- these are deviations from mass balance (= isostasy)
- various concepts of isostasy exist, i.e. of mechanisms of compensation of topographic loads
- classical: Airy, Pratt, Vening-Meinesz
modern: flexure of the lithosphere and mantle viscosity, thermal



from gravity to geodynamics



short scale geoid anomalies (degree/order 21 -200)

gravity and earth system science

Usage Three:

geoid as physically relevant reference surface

- the geoid represents the hypothetical ocean surface at rest
- the geoid makes sea level records (and height systems) worldwide comparable
- the geoid allows the conversion of GPS-heights physical heights

GOCE and ocean

Objectives:

role of oceans in climate system

Step 1: mean dynamic topography (MDT) from GOCE and altimetry

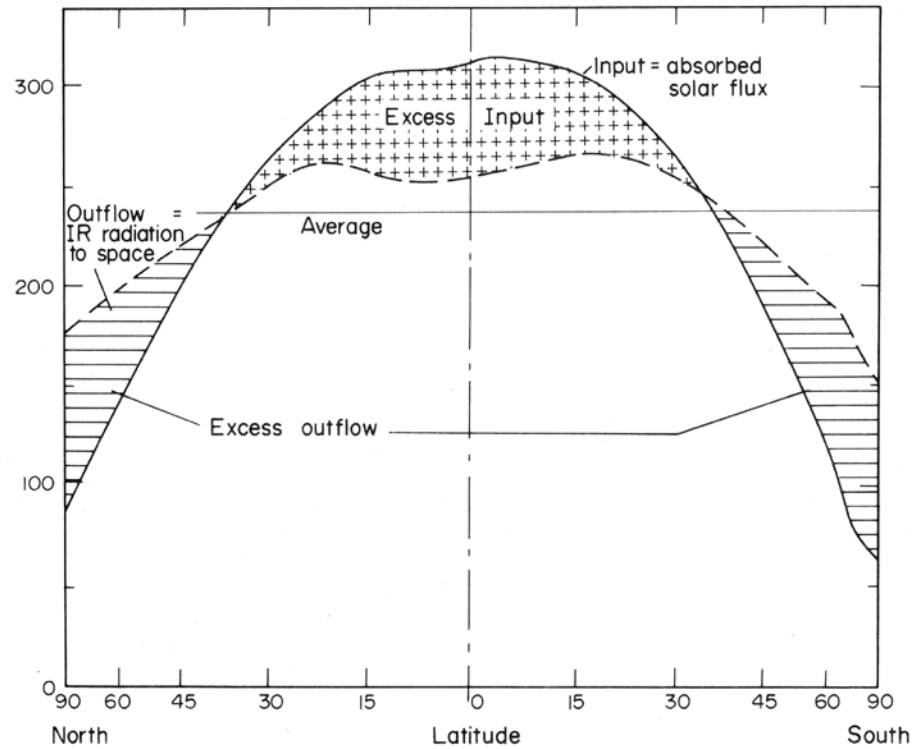
Step 2: from MDT to velocities using equations of motion

Step 3: from surface circulation to circulation at depth

Some additional results

assimilation experiments

role of oceans in climate system

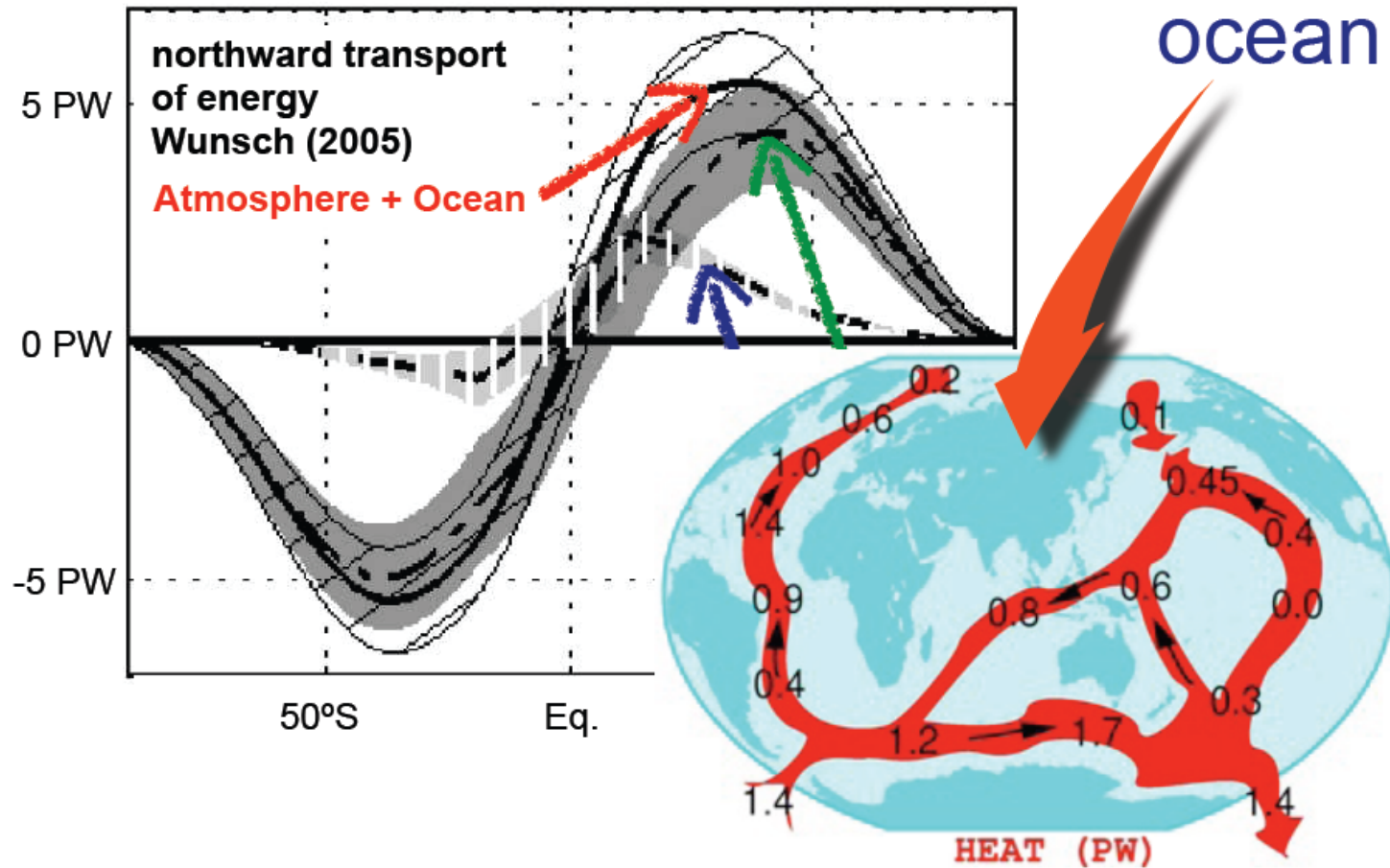


Kandel 1980

Figure 7-5. Energy gains and losses by the Earth-atmosphere system, as a function of latitude, averaged over the year (after Ellis and Vonder Haar).³

role of oceans in climate system

| heat transport in atmosphere and ocean

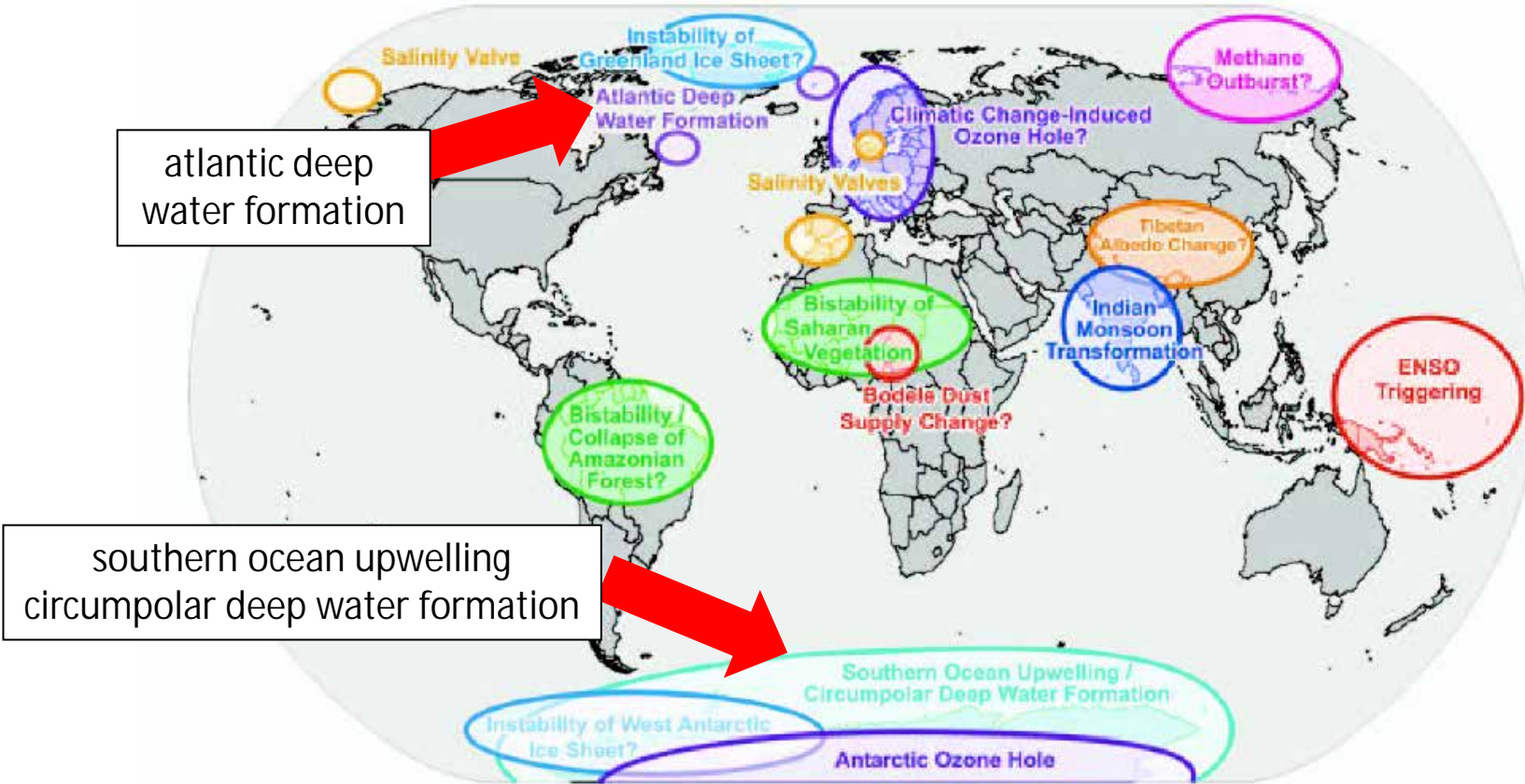


Losch, 2010

heat transport from equator region polewards:
contribution of oceans 50% (textbooks) or 20 to 30%?

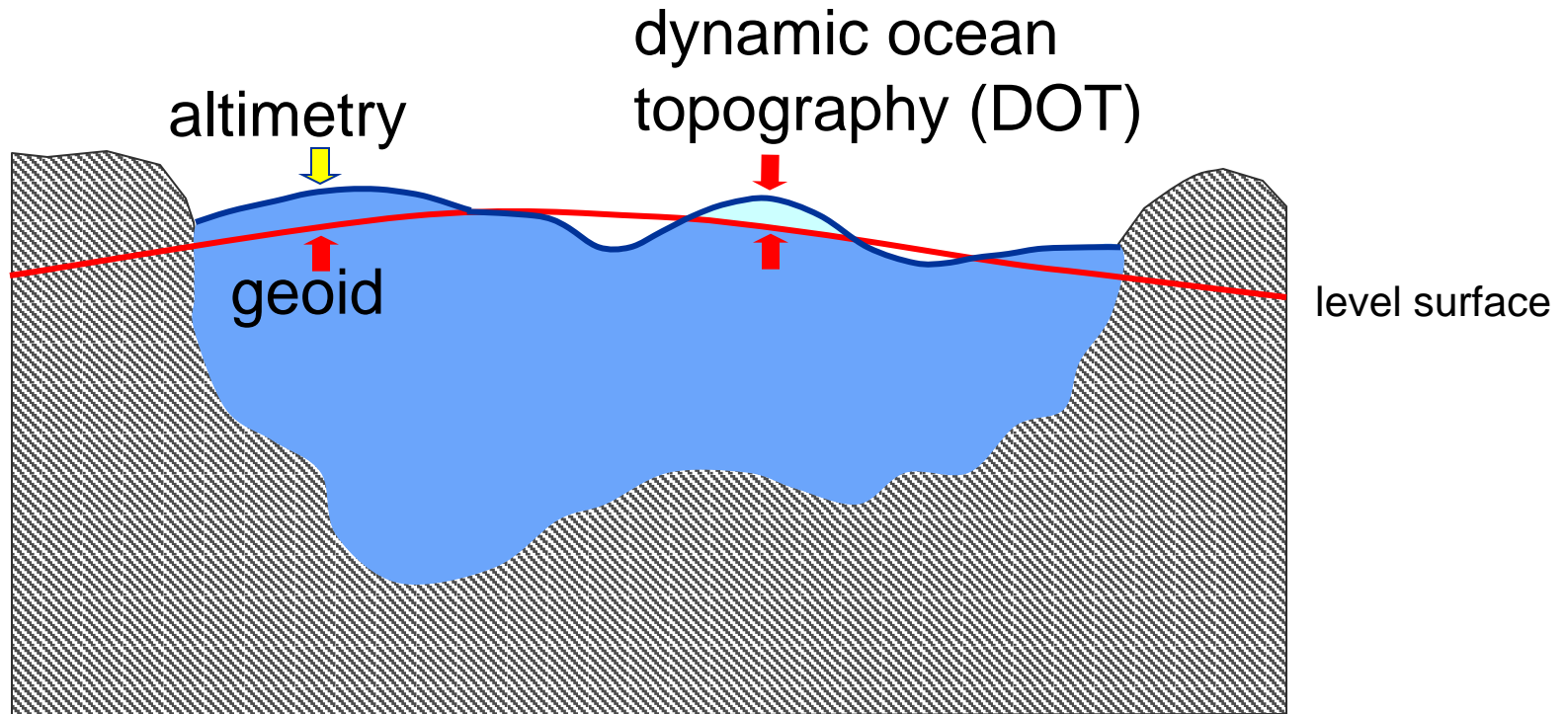
role of oceans in climate system

„tipping points“ of climate system



geodetic mean dynamic topography (MDT)

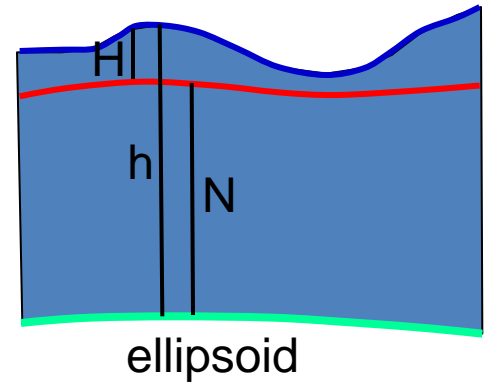
Step One



dynamic ocean topography (DOT) or mean dynamic topography (MDT): deviation of the actual mean ocean surface from the geoid (hypothetical surface of ocean at rest); size 1 to 2 m; surface circulation follows contour lines of MDT

geodetic mean dynamic topography (MDT)

$$H = \text{MDT} = h - N$$



geodetic MDT :

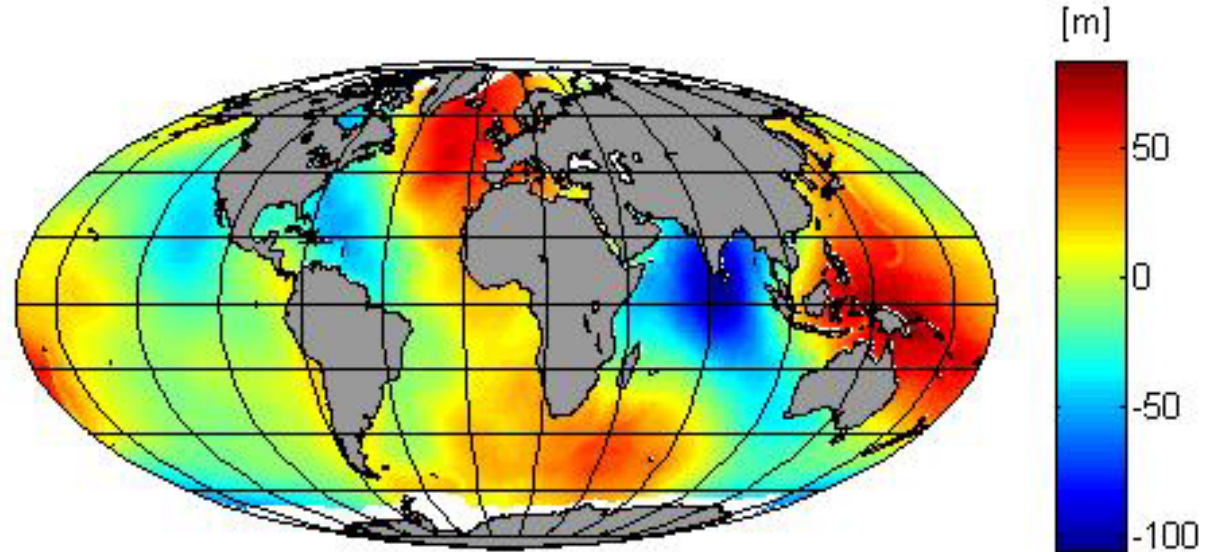
a small quantity to be derived from

two very different satellite techniques,

with cm-precision and free of systematic distortions

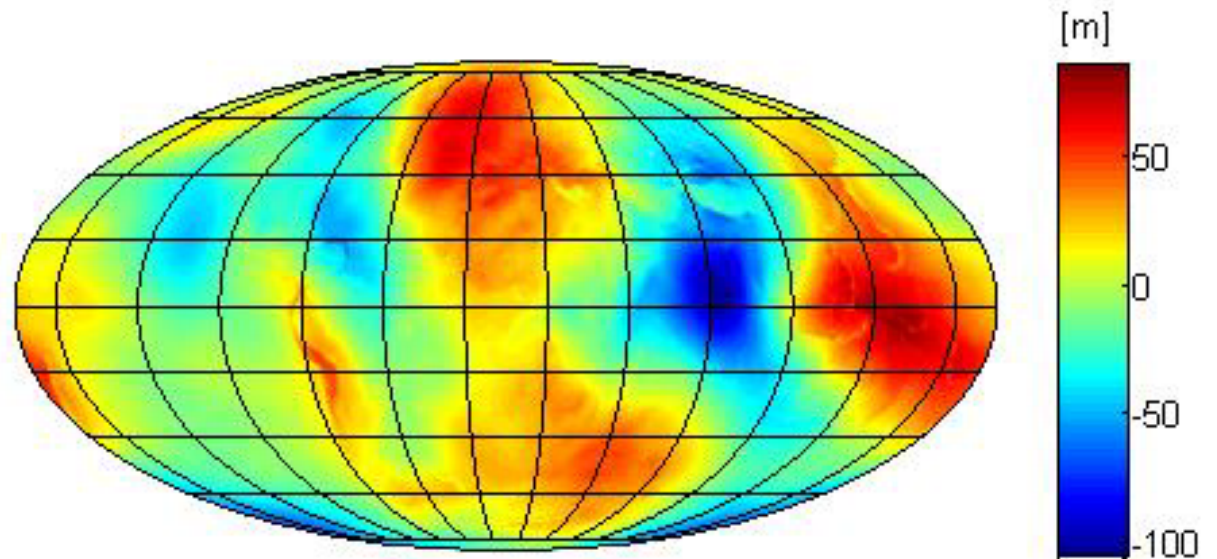
geodetic mean dynamic topography (MDT)

mean ocean surface
1992- 2010
from satellite altimetry

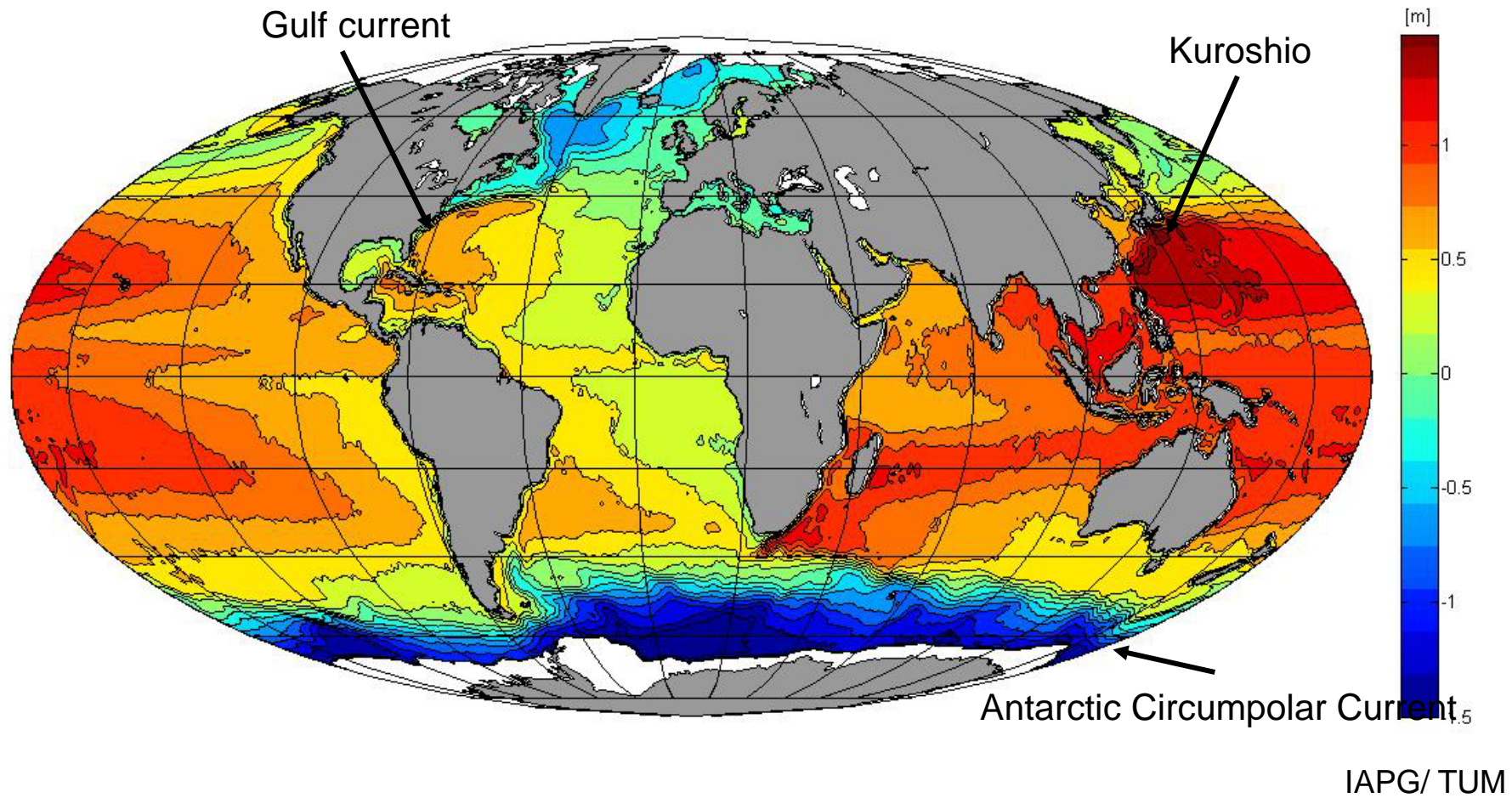


[source: W. Bosch, DGFI, 2011]

geoid
from six months
GOCE data

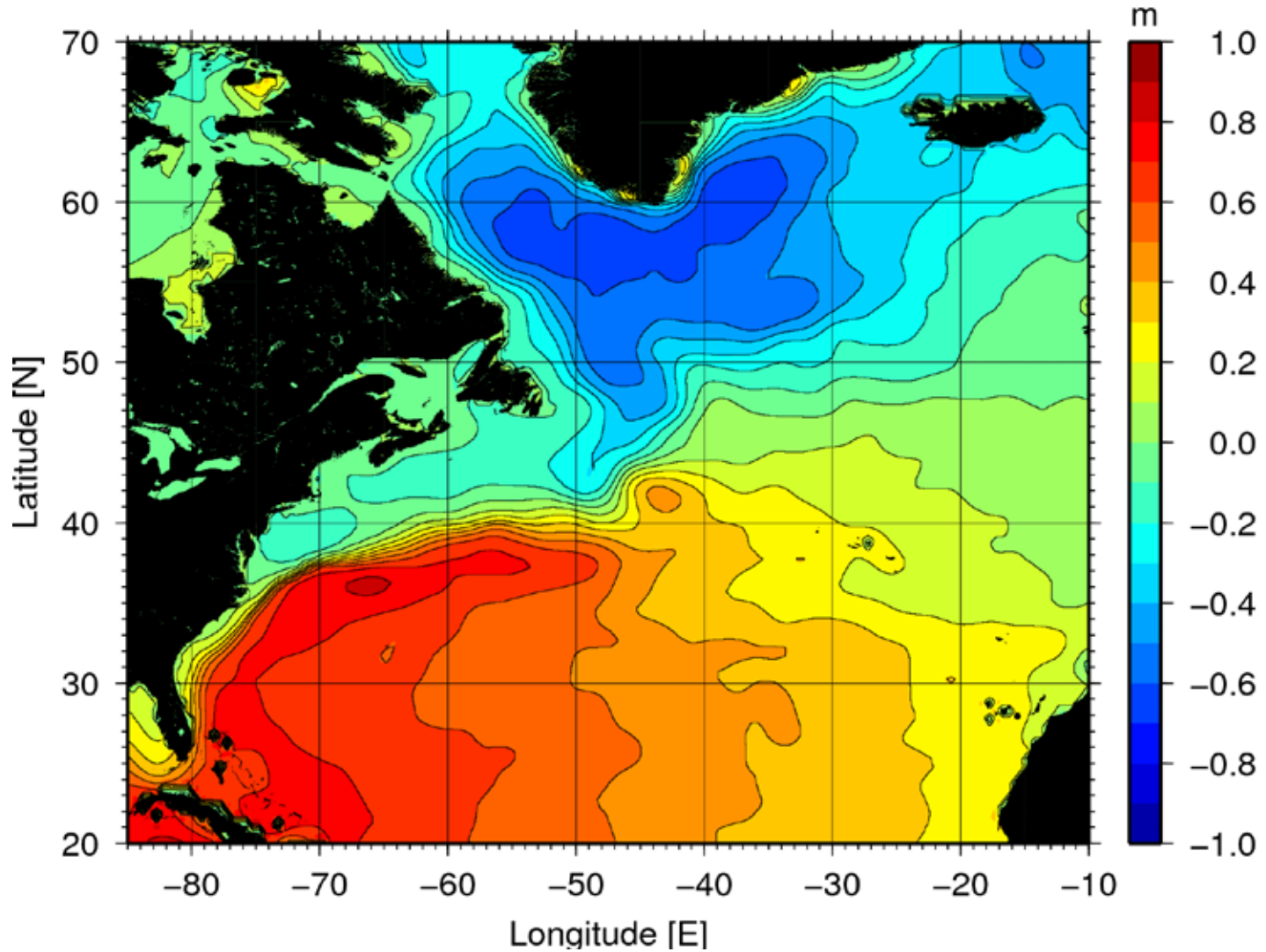


geodetic mean dynamic topography (MDT)



global mean ocean topography (in m)

geodetic mean dynamic topography (MDT)



Bingham et al., 2011

mean dynamic ocean topography in the North Atlantic

geodetic mean dynamic topography (MDT)

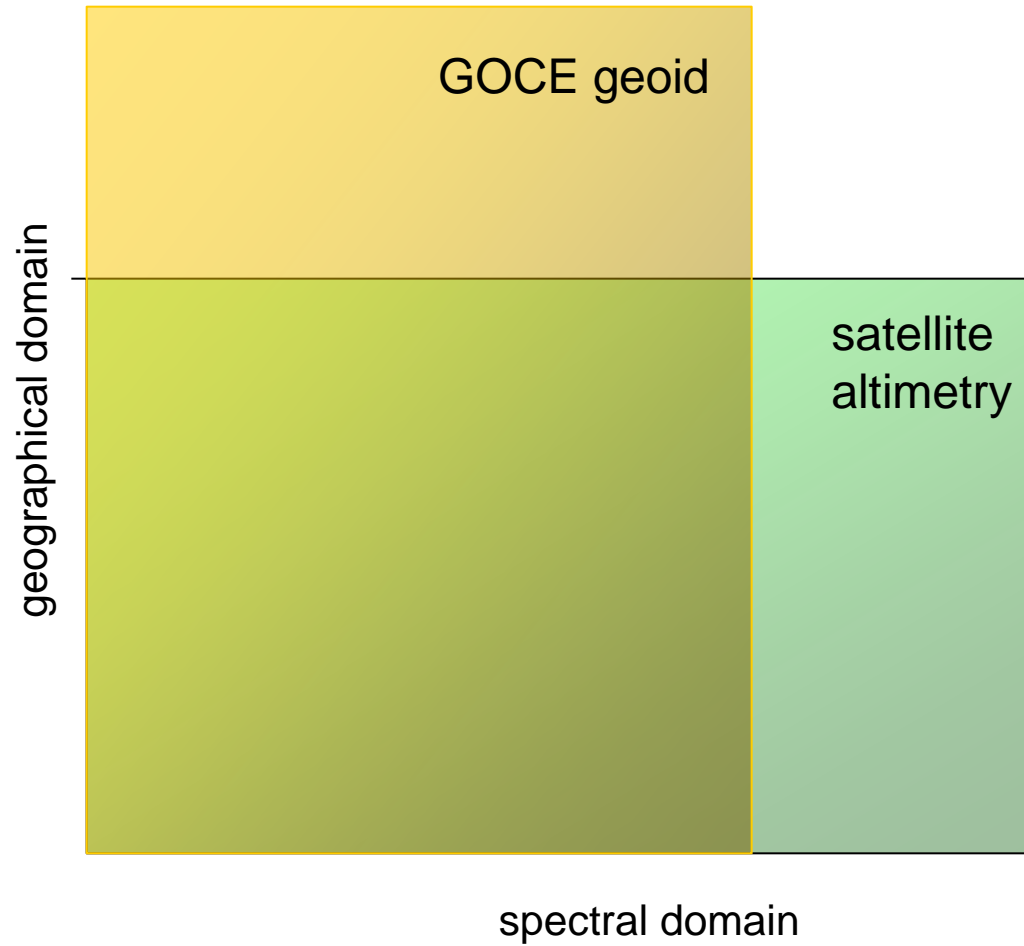
Mean ocean surface and *geoid* have to be expressed:

- in the same coordinate system
- in the same coordinate type
- with respect to the same reference ellipsoid
- in the same permanent tide system

and they have to be

- spectrally consistent (a real challenge)

geodetic mean dynamic topography (MDT)



from MDT to ocean surface circulation

Step Two

conservation of linear momentum

$$\frac{dw}{dt} + u \frac{\partial u}{\partial x} + v \frac{\partial u}{\partial y} + w \frac{\partial u}{\partial z} = -\frac{1}{r} \frac{\partial p}{\partial x} + 2Wv \sin j + F_x$$

$$\frac{dw}{dt} + u \frac{\partial v}{\partial x} + v \frac{\partial v}{\partial y} + w \frac{\partial v}{\partial z} = -\frac{1}{r} \frac{\partial p}{\partial y} - 2Wu \sin j + F_y$$

$$\frac{dw}{dt} + u \frac{\partial w}{\partial x} + v \frac{\partial w}{\partial y} + w \frac{\partial w}{\partial z} = -\frac{1}{r} \frac{\partial p}{\partial z} + 2Wu \cos j - g + F_z$$

expressed in a local (spherical) coordinate system {east, north, up}
and rotating with the earth, p pressure, Ω earth angular velocity,
 g gravity, F forces such as wind stress or tides

assumed:

$$w \ll v \quad 2W \cos j \ll w \gg 0$$

from MDT to ocean surface circulation

Scaling the Equations: The Geostrophic Approximation

We wish to simplify the equations of motion to obtain solutions that describe the deep-sea conditions well away from coasts and below the Ekman boundary layer at the surface. To begin, let's examine the typical size of each term in the equations in the expectation that some will be so small that they can be dropped without changing the dominant characteristics of the solutions. For interior, deep-sea conditions, typical values for distance L , horizontal velocity U , depth H , Coriolis parameter f , gravity g , and density ρ are:

$$L \approx 10^6 \text{ m} \quad H_1 \approx 10^3 \text{ m} \quad f \approx 10^{-4} \text{ s}^{-1} \quad \rho \approx 10^3 \text{ kg/m}^3$$

$$U \approx 10^{-1} \text{ m/s} \quad H_2 \approx 1 \text{ m} \quad \rho \approx 10^3 \text{ kg/m}^3 \quad g \approx 10 \text{ m/s}^2$$

where H_1 and H_2 are typical depths for pressure in the vertical and horizontal.

From these variables we can calculate typical values for vertical velocity W , pressure P , and time T :

$$\frac{\partial W}{\partial z} = - \left(\frac{\partial U}{\partial x} + \frac{\partial v}{\partial y} \right)$$

$$\frac{W}{H_1} = \frac{U}{L}; \quad W = \frac{UH_1}{L} = \frac{10^{-1} 10^3}{10^6} \text{ m/s} = 10^{-4} \text{ m/s}$$

$$P = \rho g H_1 = 10^3 10^1 10^3 = 10^7 \text{ Pa}; \quad \partial p / \partial x = \rho g H_2 / L = 10^{-2} \text{ Pa/m}$$

$$T = L / U = 10^7 \text{ s}$$

The momentum equation for vertical velocity is therefore:

$$\frac{\partial w}{\partial t} + u \frac{\partial w}{\partial x} + v \frac{\partial w}{\partial y} + w \frac{\partial w}{\partial z} = -\frac{1}{\rho} \frac{\partial p}{\partial z} + 2\Omega u \cos \varphi - g$$

$$\frac{W}{T} + \frac{UW}{L} + \frac{UW}{L} + \frac{W^2}{H} = \frac{P}{\rho H_1} + fU - g$$

$$10^{-11} + 10^{-11} + 10^{-11} + 10^{-11} = 10^{-5} + 10^{-5} - 10$$

and the only important balance in the vertical is hydrostatic:

$$\frac{\partial p}{\partial z} = -\rho g \quad \text{Correct to } 1:10^6.$$

The momentum equation for horizontal velocity in the x direction is:

$$\frac{\partial u}{\partial t} + u \frac{\partial u}{\partial x} + v \frac{\partial u}{\partial y} + w \frac{\partial u}{\partial z} = -\frac{1}{\rho} \frac{\partial p}{\partial x} + fv$$

$$10^{-8} + 10^{-8} + 10^{-8} + 10^{-8} = 10^{-5} + 10^{-5}$$

Thus the Coriolis force balances the pressure gradient within one part per thousand. This is called the *geostrophic balance*, and the *geostrophic equations* are:

$$\frac{1}{\rho} \frac{\partial p}{\partial x} = fv; \quad \frac{1}{\rho} \frac{\partial p}{\partial y} = -fu; \quad \frac{1}{\rho} \frac{\partial p}{\partial z} = -g$$

This balance applies to oceanic flows with horizontal dimensions larger than roughly 50 km and times greater than a few days.

scaling of the momentum equations
leads to the
geostrophic balance

Robert H Stewart:
Introduction to Physical Oceanography, 2008

from MDT to ocean surface circulation

$$u \frac{\partial u}{\partial x} + v \frac{\partial u}{\partial y} + w \frac{\partial u}{\partial z} = -\frac{1}{r} \frac{\partial p}{\partial x} + 2Wv \sin j + F_x$$

$$u \frac{\partial v}{\partial x} + v \frac{\partial v}{\partial y} + w \frac{\partial v}{\partial z} = -\frac{1}{r} \frac{\partial p}{\partial y} - 2Wu \sin j + F_y$$

$$u \frac{\partial w}{\partial x} + v \frac{\partial w}{\partial y} + w \frac{\partial w}{\partial z} = -\frac{1}{r} \frac{\partial p}{\partial z} + 2Wu \cos j - g + F_z$$

geostrophic balance:

pressure gradient = - Coriolis acceleration

and

hydrostatic (pressure) equation

from MDT to ocean surface circulation

$$\nabla p = -g r \nabla z - f$$

$$g \frac{\nabla z}{\nabla x} = -2W \sin j v \quad \text{or} \quad \frac{\nabla H}{\nabla x} = -\frac{f}{g} v$$

$$g \frac{\nabla z}{\nabla y} = 2W \sin j u \quad \text{or} \quad \frac{\nabla H}{\nabla y} = \frac{f}{g} u$$

establishes the relationship between sea surface slope

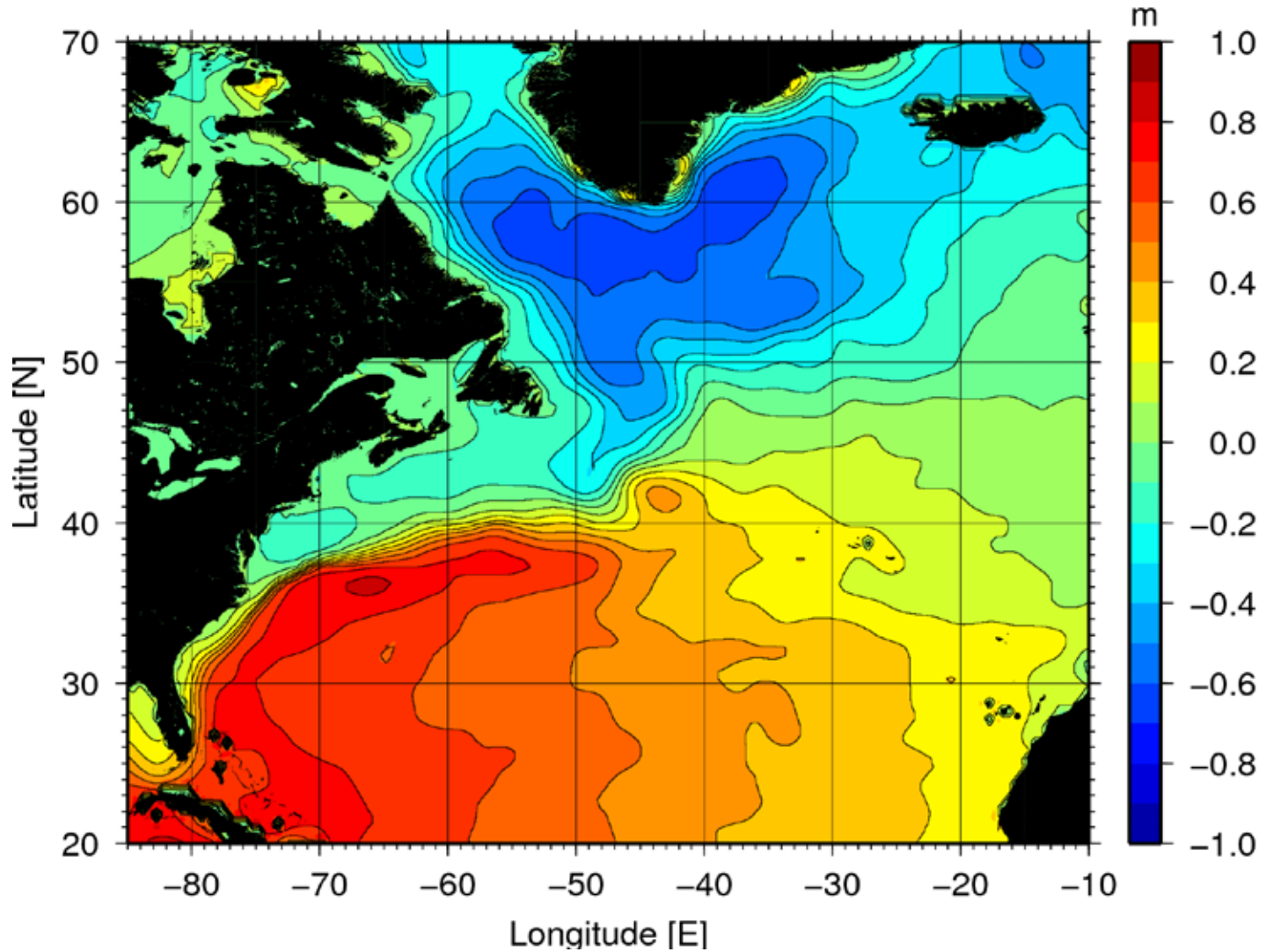
$$\{\delta H / \delta x, \delta H / \delta y\}$$

and surface ocean circulation (velocity);

the motion is perpendicular to the slope i.e. parallel to the contour lines of DOT;

the slope is proportional to the velocity

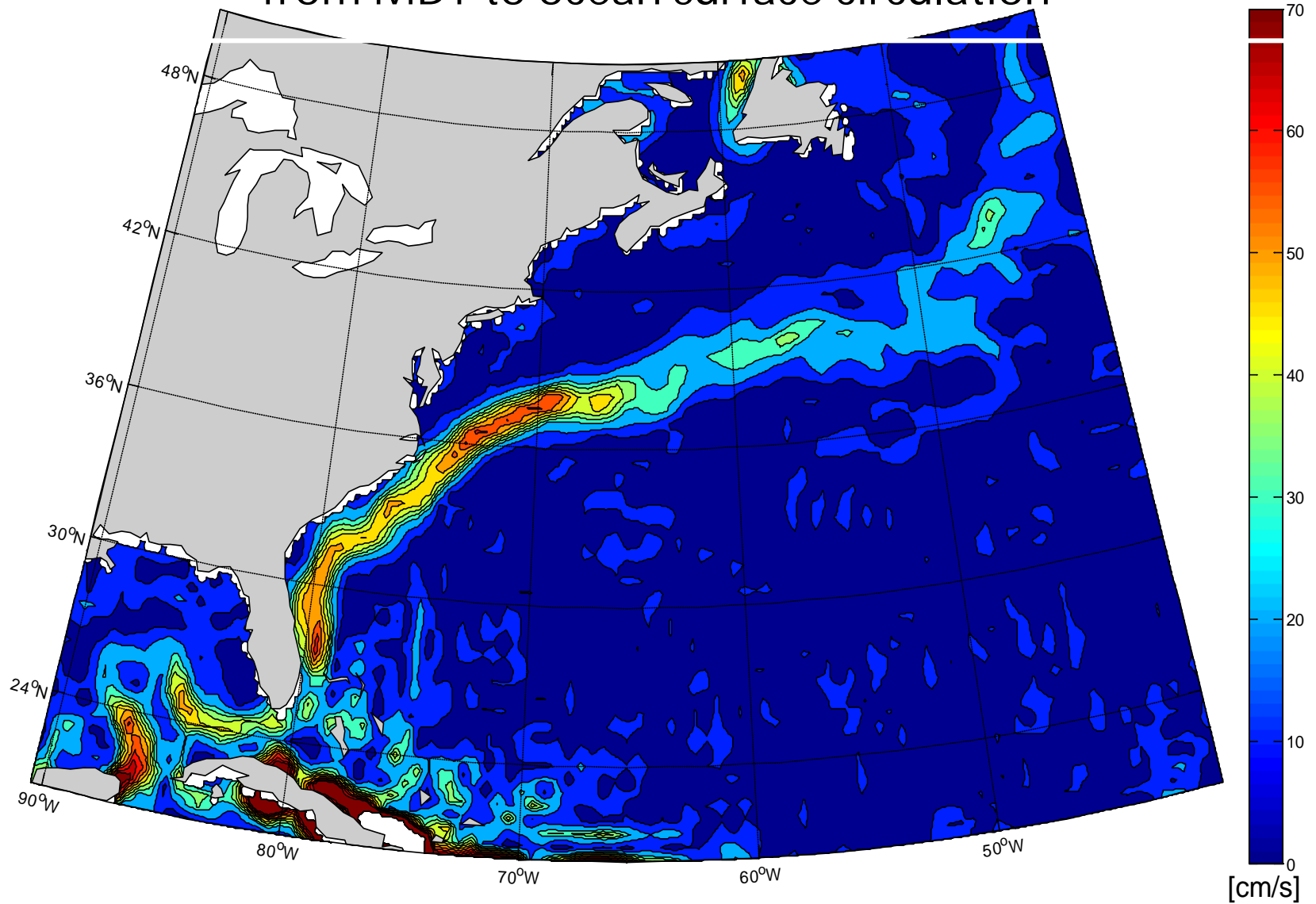
from MDT to ocean surface circulation



Bingham et al., 2011

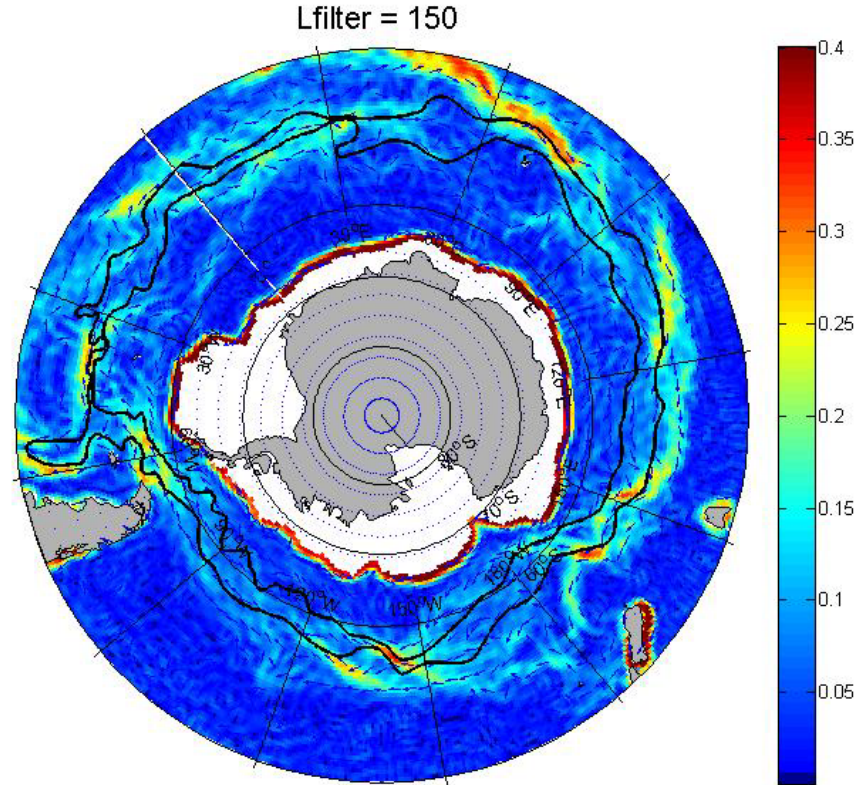
mean dynamic ocean topography in the North Atlantic

from MDT to ocean surface circulation



geostrophic surface velocities in the North Atlantic
from GOCE and altimetric MSS

from MDT to ocean surface circulation



Geostrophic surface velocities in the area of the ACC
from a GOCE geoid surface (D/O 150)
and an altimetric MSS (DGFI2010)

Front systems (in black) derived from oceanographic in-situ data

from ocean surface to circulation at depth

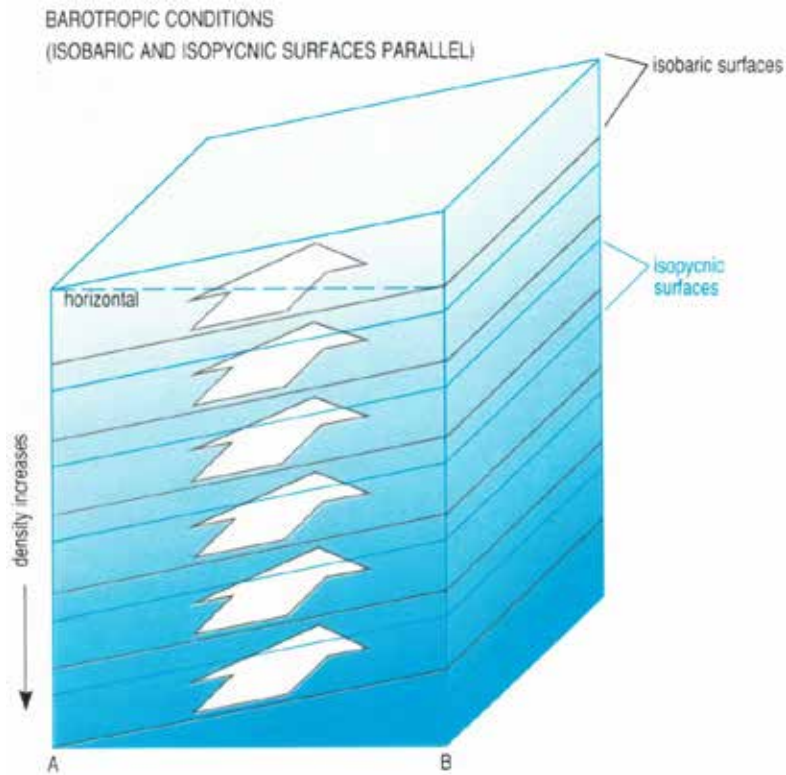
Step Three

A connection between GOCE, in-situ data (Argo, drifters...) and GRACE:
from surface circulation to ocean velocity at depth
by measuring temperature and salinity profiles
(or vertical changes of ocean pressure)

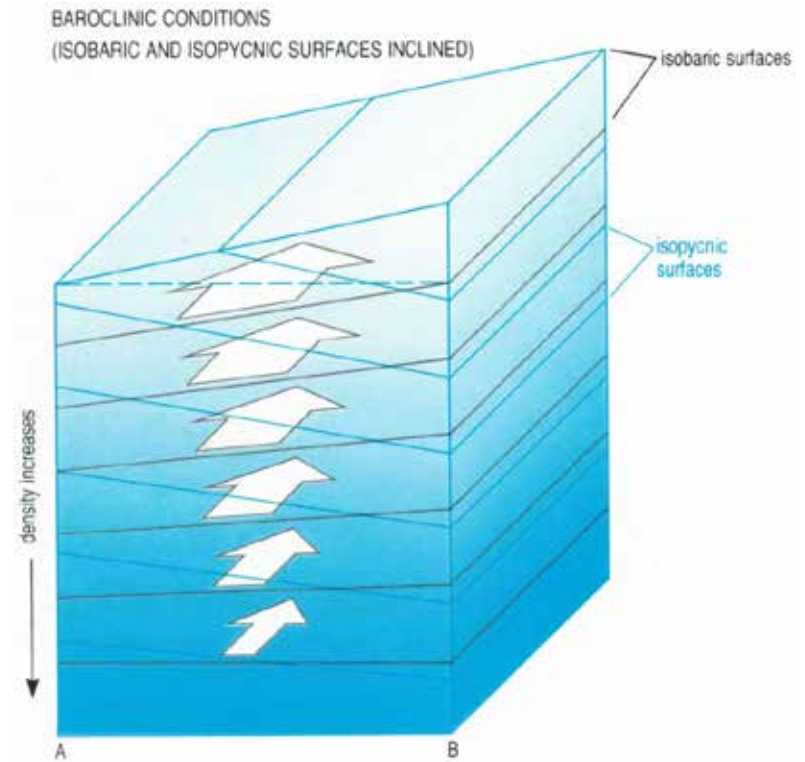
$$u = -\frac{1}{f\rho} \frac{\partial}{\partial y} \int_{\text{depth}}^0 g(j, z) \rho(z) dz - \frac{g}{f} \frac{\partial H}{\partial y}$$

$$v = -\frac{1}{f\rho} \frac{\partial}{\partial x} \int_{\text{depth}}^0 g(j, z) \rho(z) dz + \frac{g}{f} \frac{\partial H}{\partial x}$$

from ocean surface to circulation at depth

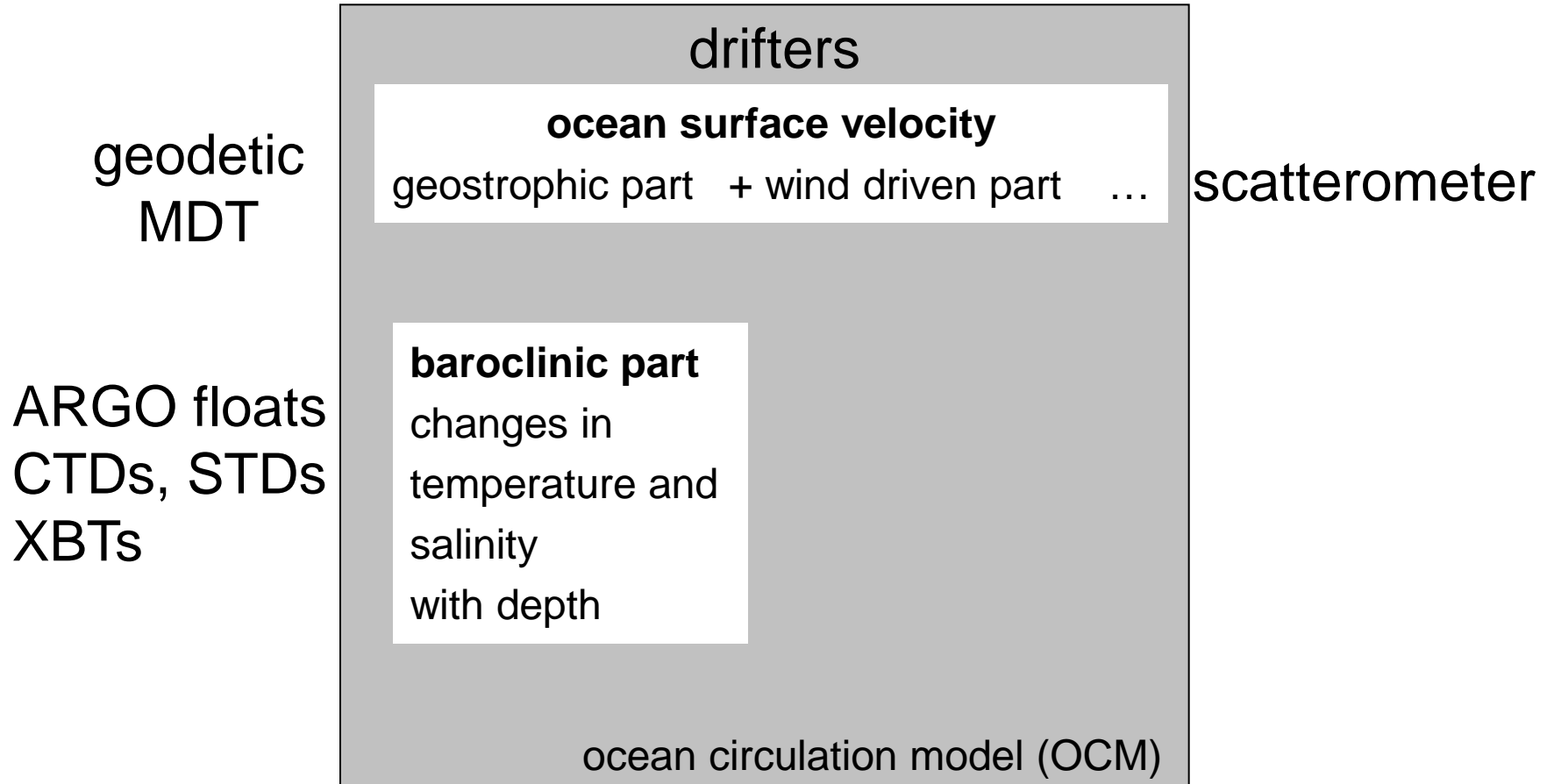


barotropic flow:
isobaric and isopycnic surfaces
are parallel



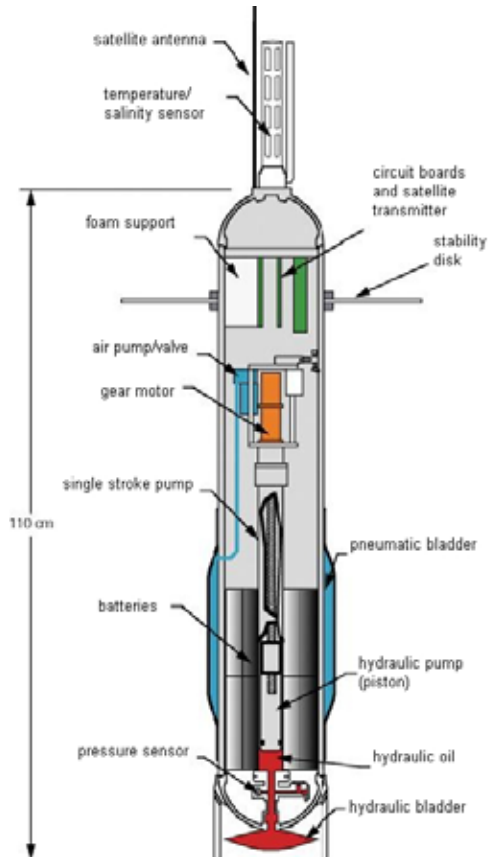
baroclinic flow:
isobaric surfaces are inclined
to isopycnic surfaces

from ocean surface to circulation at depth



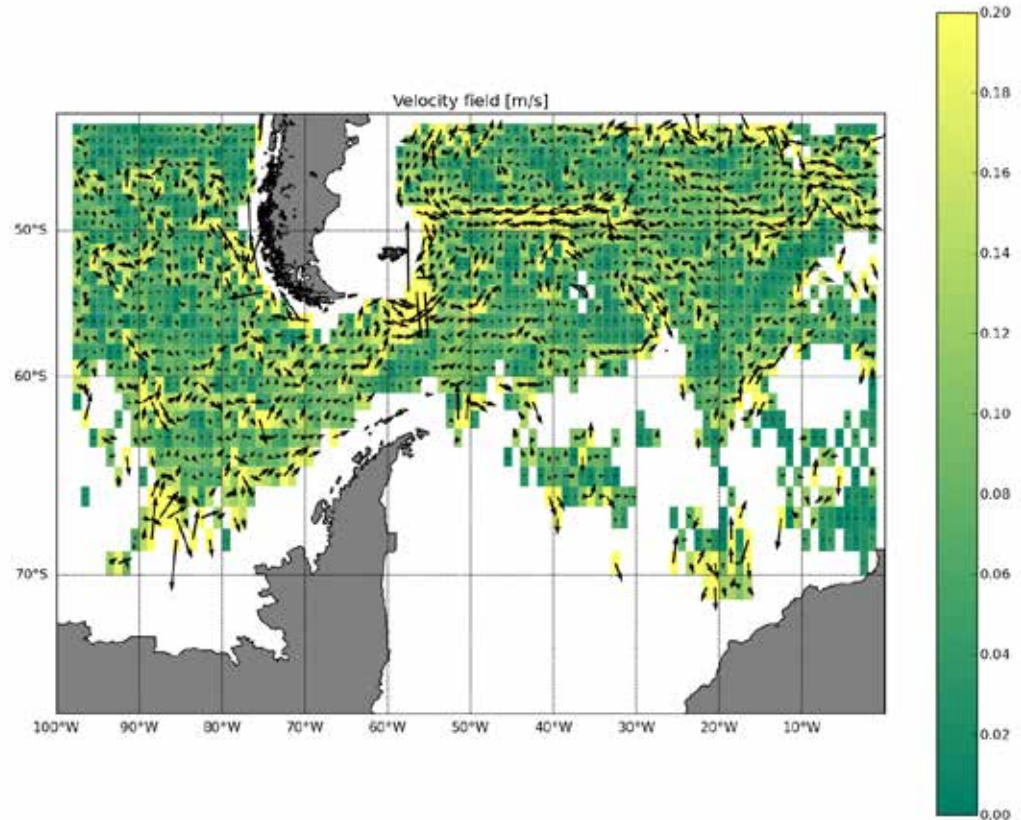
from ocean surface to circulation at depth

ARGO float



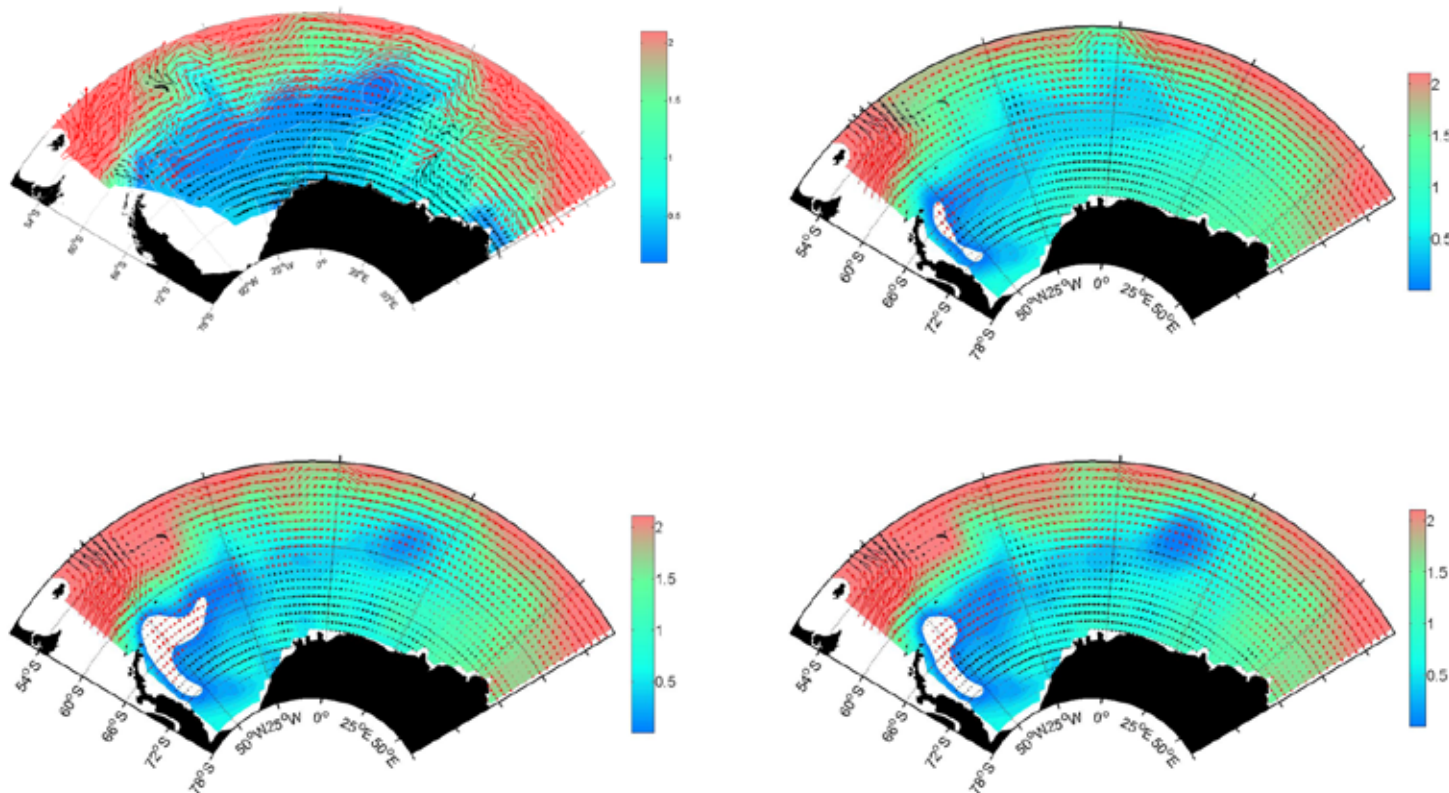
source: IMOS,
Australian Government

ocean surface velocities from ARGO data



Tribet
Environmental Engineering, TUM

The Weddell gyre flow



In-situ temperature at 800 m depth. Composite from the ARGO data (1999 to 2010) (upper left). As result of model only (upper right), assimilation of geodetic DOT filtered up to 241 km (lower left) and of geodetic DOT filtered up to 121 km (lower right).

conclusions

- Not discussed

 - solid earth physics: joint inversion with seismic tomography

 - unification of sea level records

 - conversion of GPS-heights to physical heights

- geodetic MDT: from space, globally consistent, no ocean data

- spatial resolution must be further improved (Rossby radius)

- spectral consistency is a challenge

- from surface circulation to circulation at depth

- GOCE provides high resolution reference surface

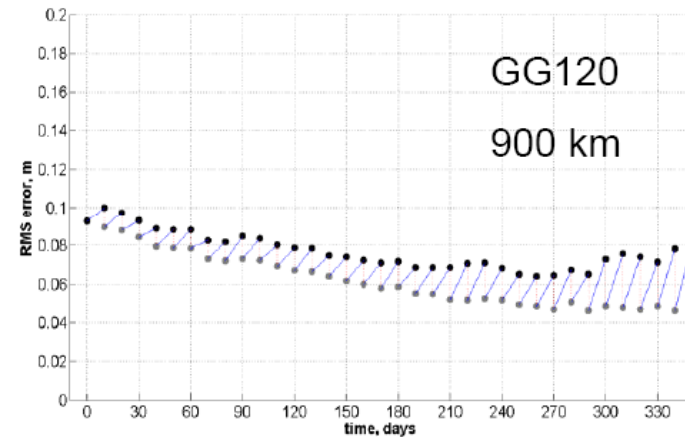
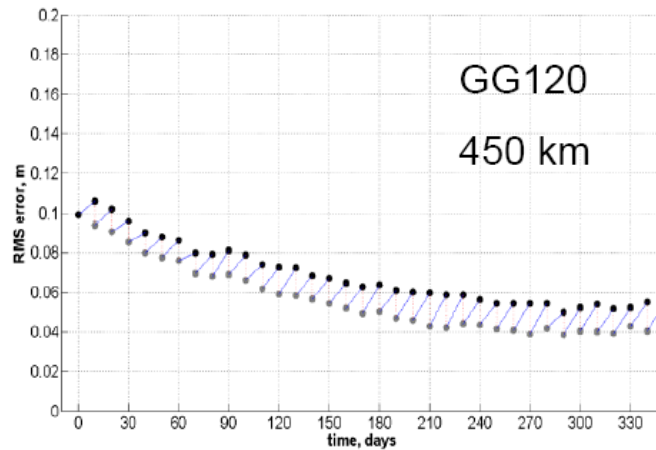
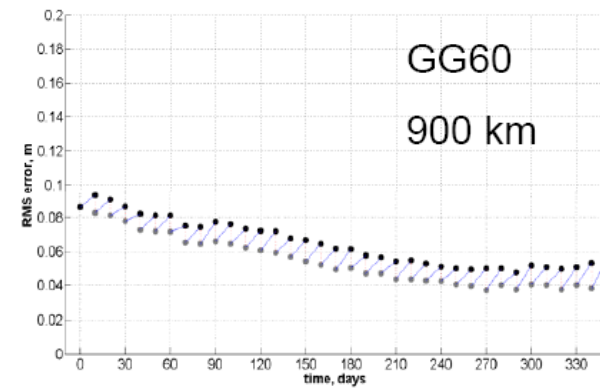
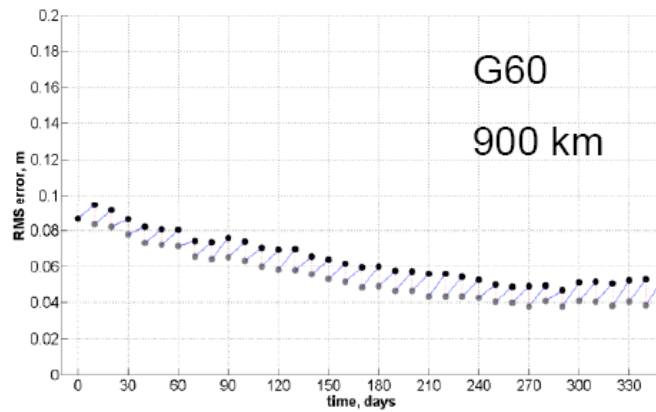
 - focus of future missions can therefore be on temporal variations

Reference on GOCE:

special issue of Journal of Geodesy, vol 85-11, 201

from ocean surface to circulation at depth

RMS errors with respect to assimilated data

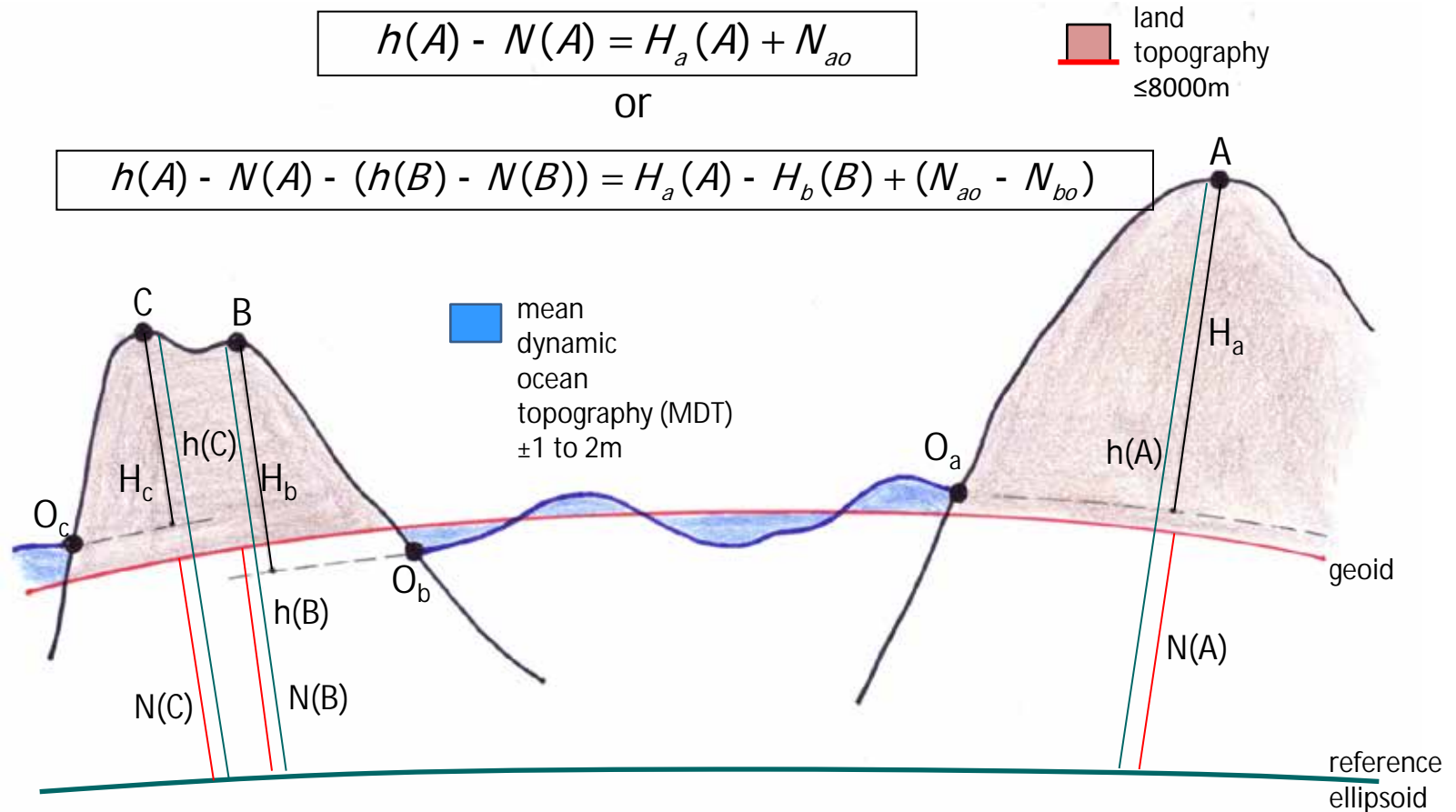


height datum unification: principle

$$h(A) - N(A) = H_a(A) + N_{ao}$$

or

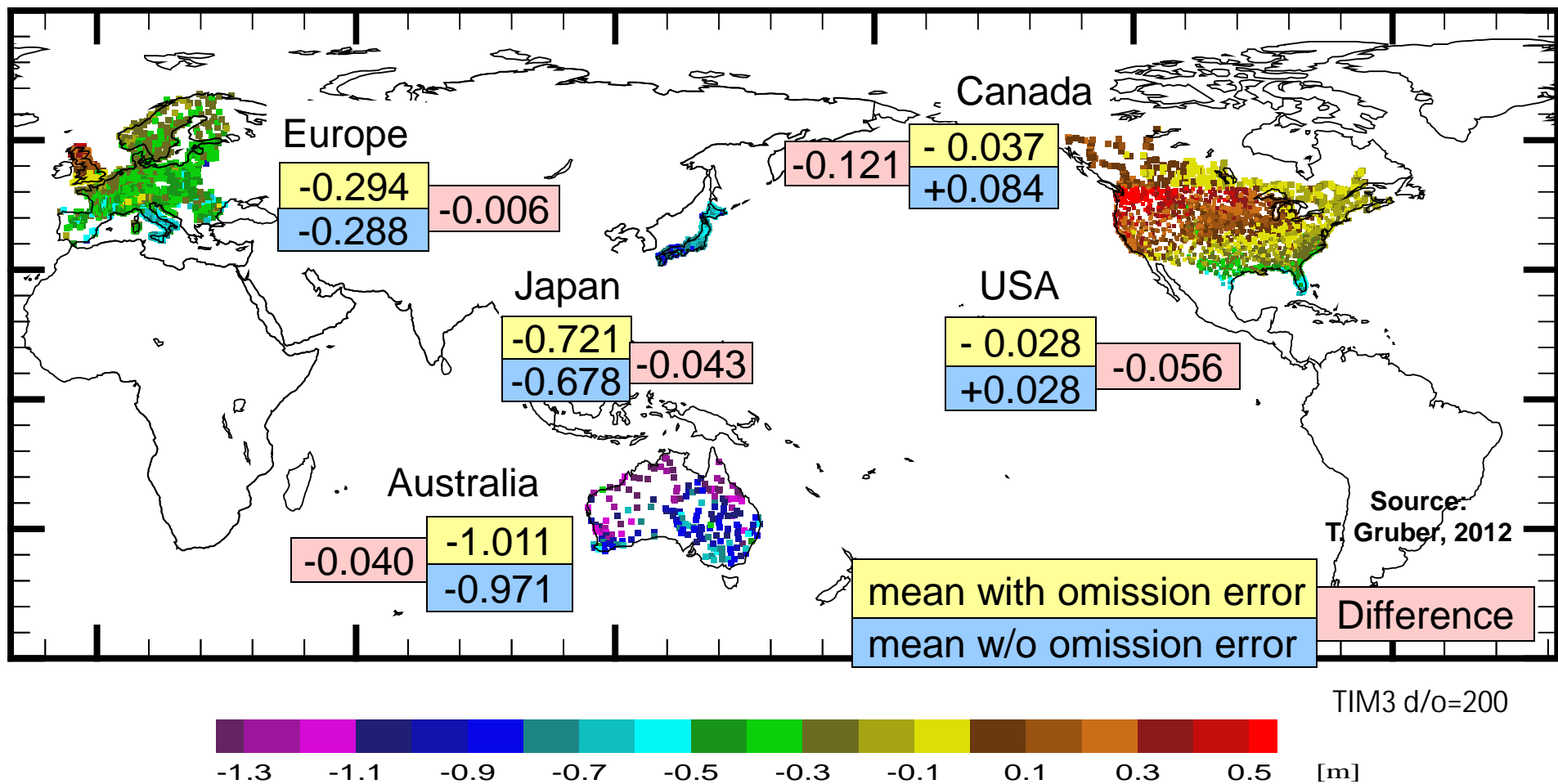
$$h(A) - N(A) - (h(B) - N(B)) = H_a(A) - H_b(B) + (N_{ao} - N_{bo})$$



theoretical results

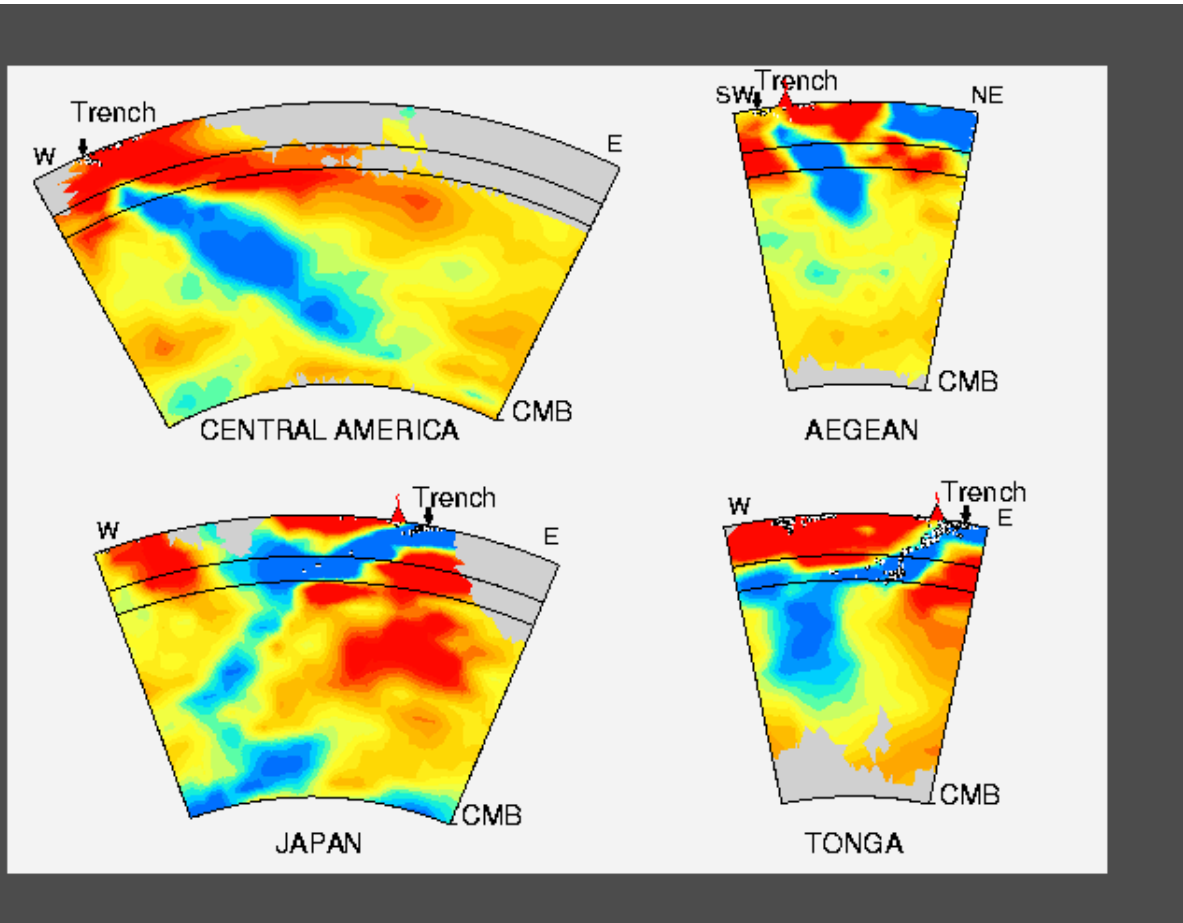
Preliminary tests show:

Modeling of the omission part with EGM2008 in well surveyed countries leaves an uncertainty of below 10cm (see: Gruber)



solid Earth observation

most prominent observation technique in solid earth studies: seismic tomography

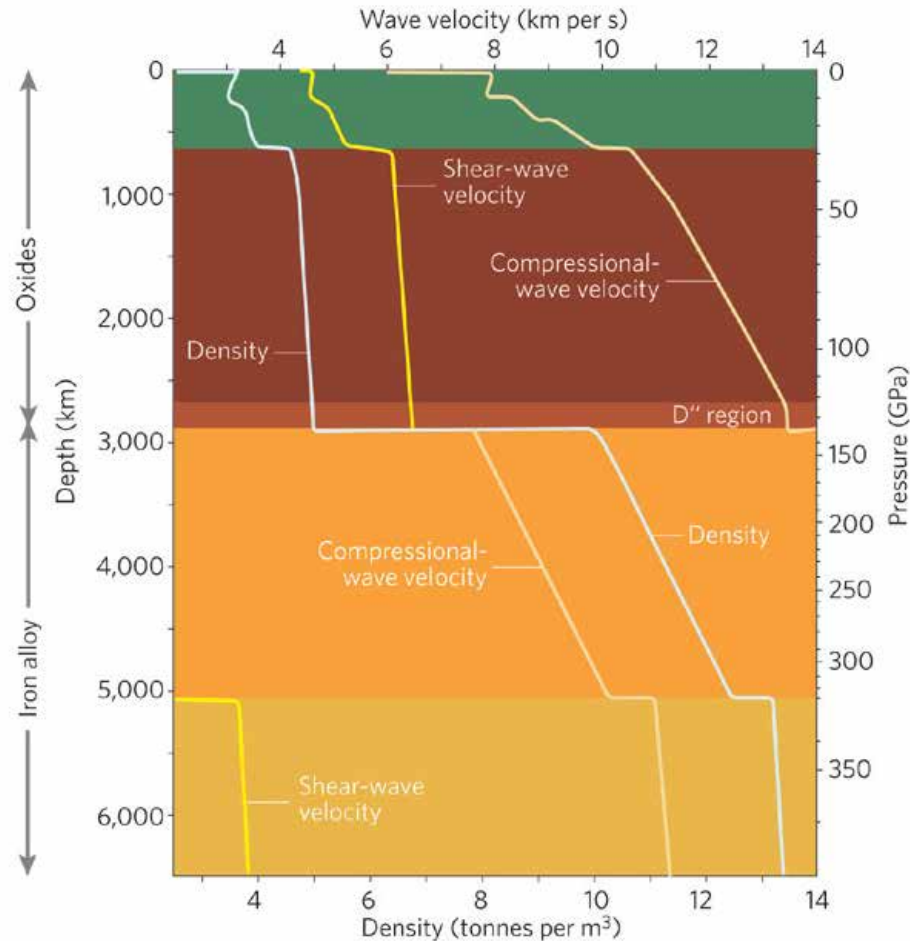


van der Hilst, Grand, Masters, Trampert, 2004 (?)

blue = high seismic velocity red = low seismic velocity

solid Earth observation

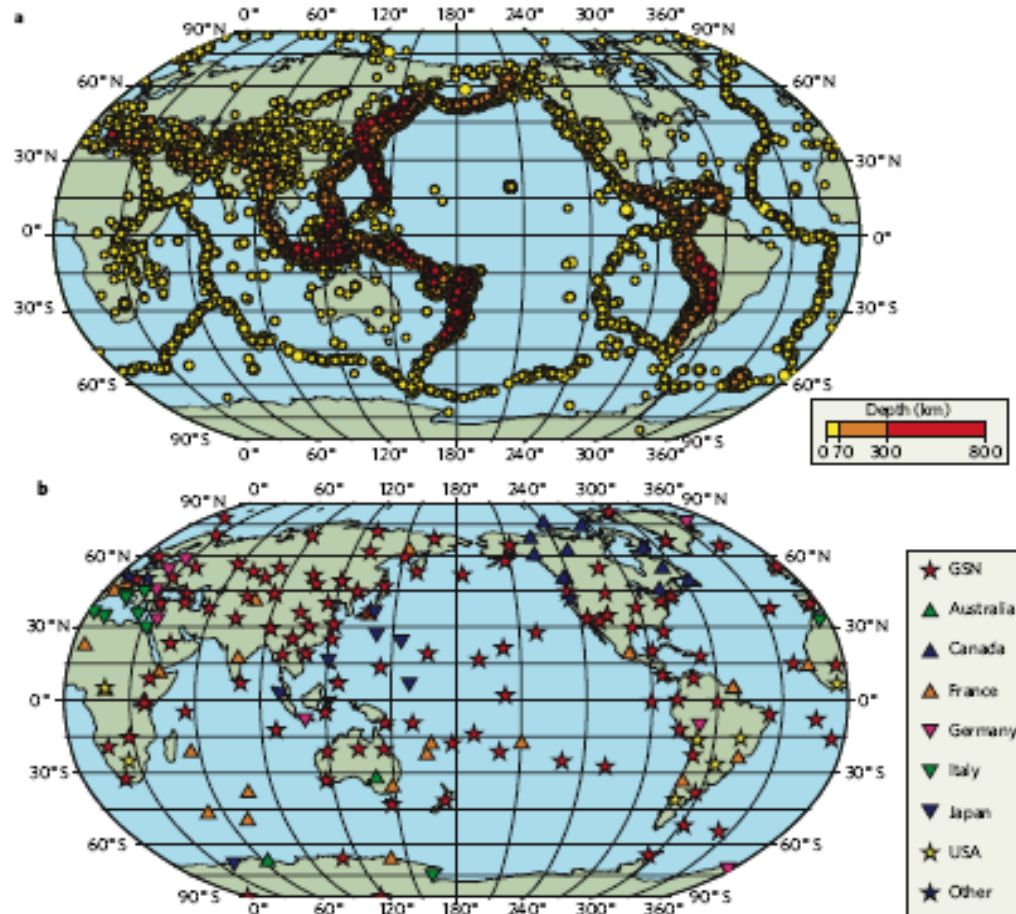
velocity of shear waves and compressional waves
as well as density as a function of depth



from gravity to geodynamics

signal source are earthquakes (at plate boundaries)

measured with seismometers in a global network (mostly on land)



from gravity to geodynamics

seismic tomography:

- sources: earthquakes (at plate boundaries)
- seismometers: global networks (mostly on land)
- output of inversion:

3D images of shear wave velocities v_s
and/or of compressional wave velocities v_p

discussion:

inversion is not unbiased

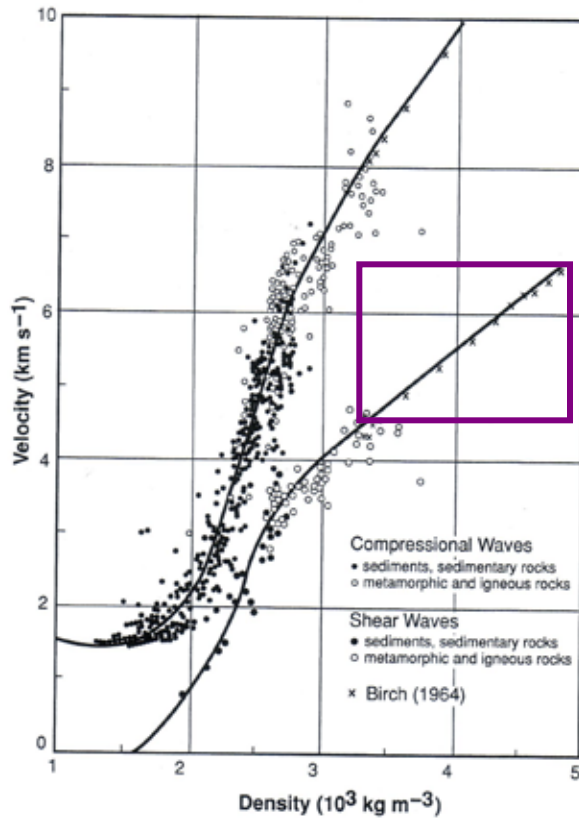
translation of the v_s and v_p to density

depends also on shear modulus and bulk modulus

i.e. it is non unique

from gravity to geodynamics

the difficulty of converting seismic velocities to density:
the answer: joint inversion with gravity and geoid



$$a = v_p = \sqrt{\frac{K + \frac{4}{3}m}{r}}$$

$$b = v_s = \sqrt{\frac{m}{r}}$$

$r = \text{density}$,

$m = \text{shear modulus}$

$K = \text{bulk modulus}$

Birch's law :

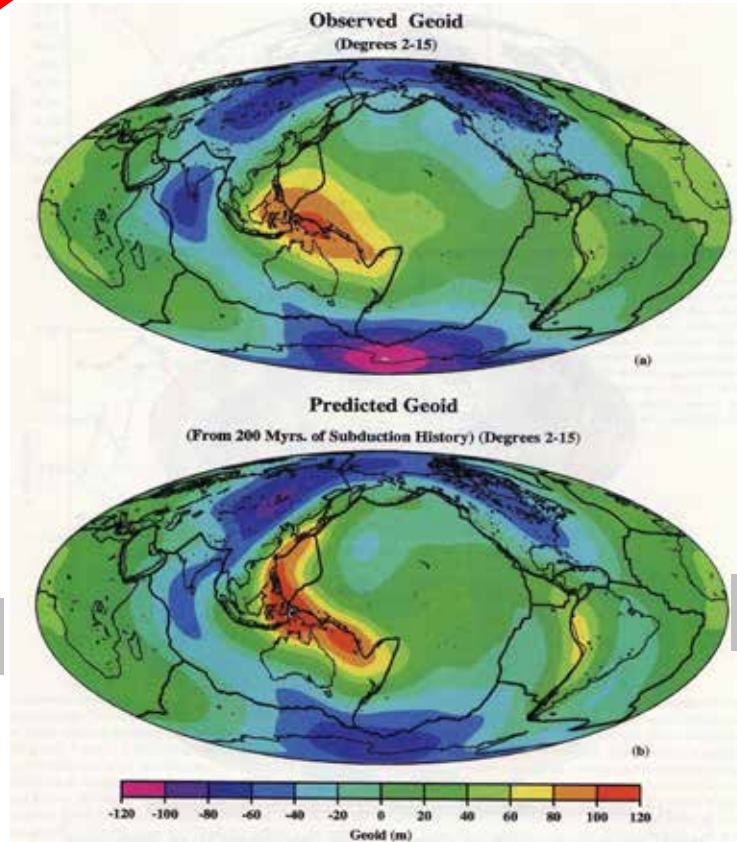
$$v = ar + b$$

from gravity to geodynamics

seismology

magnetic field

gravity and geoid



crustal motion

topography

laboratory research

(pressure, temperature, composition)

from: Lithgow-Bertelloni & Richards, 1998 in Rev. of Geophysics

from gravity to geodynamics

basic equations of mantle convection

$$\mathbf{0} = \nabla \cdot \mathbf{u}$$

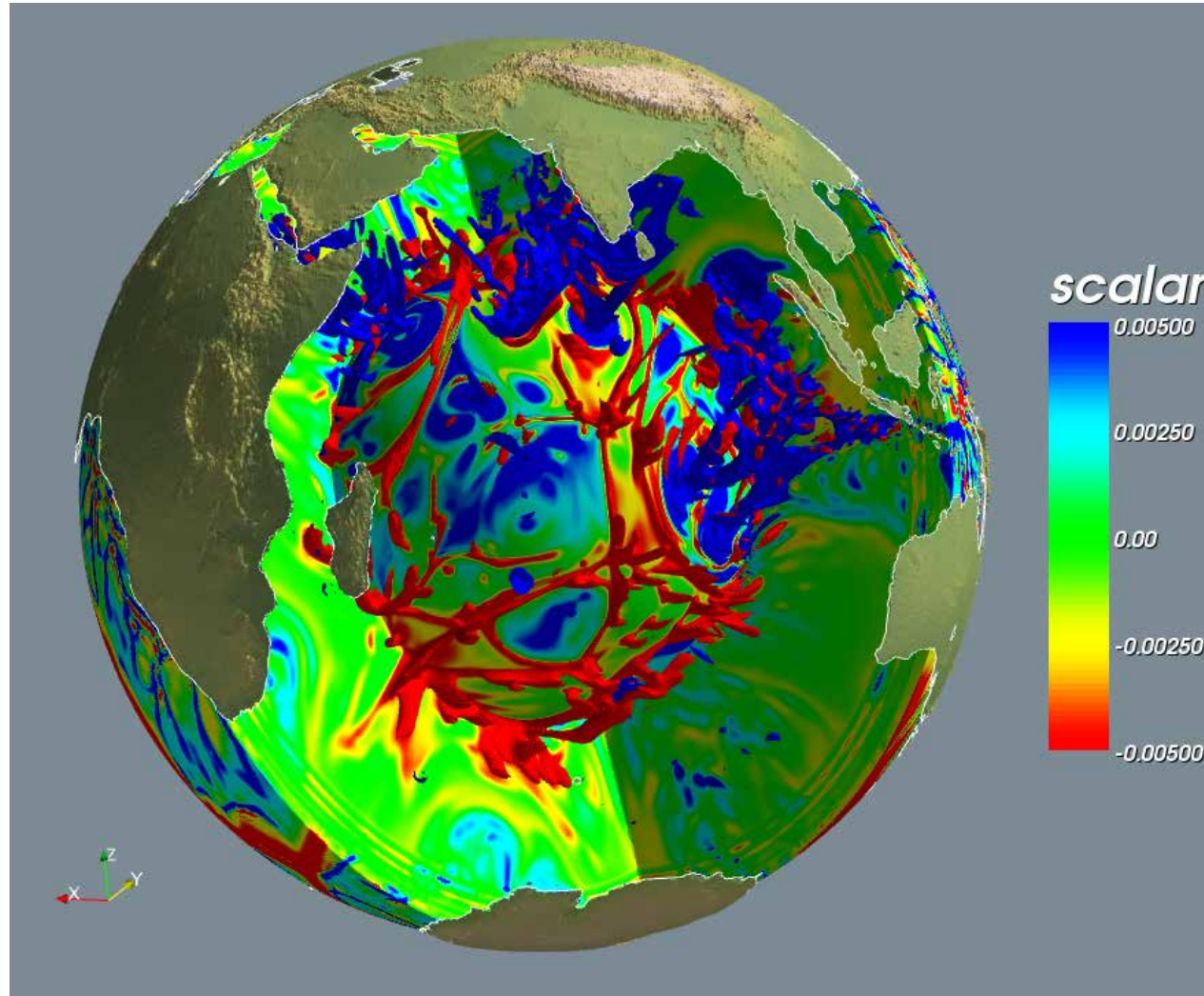
$$\mathbf{0} = -\nabla p + \nabla \cdot (\nu \nabla \mathbf{u}) + R(\bar{T} - T)\hat{\mathbf{k}}$$

$$\frac{\partial T}{\partial t} + \mathbf{u} \cdot \nabla T = \nabla^2 T + h$$

conservation of mass, linear momentum and energy

from gravity to geodynamics

global geodynamic Earth model



source: H-P Bunge